A finite element method to solve the compressible Navier-Stokes equations with turbulence modelling

Samuel Boivin

INRIA

UNITE DE RECHERCHE
INRIA-ROCQUENCOURT

Institut National
de Recherche
en Informatique
et en Automatique

Domaine de Voluceau
Rocquencourt
B.P 105
78153 Le Chesnay Cedex
France
Tél. (1) 39 63 55 11

Rapports de Recherche

N° 923

Programme 7

A FINITE ELEMENT METHOD TO SOLVE THE COMPRESSIBLE NAVIER-STOKES EQUATIONS WITH TURBULENCE MODELLING.

Sylvain BOIVIN

Novembre 1988

RR_0923

A FINITE ELEMENT METHOD TO SOLVE THE COMPRESSIBLE NAVIER-STOKES EQUATIONS WITH TURBULENCE MODELLING.

Sylvain Boivin
(Dept. de mathématiques, Université Laval, Canada, G1K 7P4
and INRIA-Menusin, 78153 Le Chesnay, France)

Abstract :

A new computer code solving the compressible Navier-Stokes equations is described. The code solve the two-dimensional (2-D), time-dependant equations using the finite element method. Filtering methods are used on gradients of convection terms in order to ensure stability. Two turbulence models are integrated into the code to compare, evaluate, and ultimately improve model performance.

The results of numerical experiments for the flow around a NACA0012 airfoil and a simplified version of the Hermes space shutle will be presented in order to show the possibilities of the methods used.

UNE METHODE NUMERIQUE DE TYPE ELEMENT FINIES POUR RESOUDRE LES EQUATIONS DE NAVIER-STOKES COMPRESSIBLE AVEC MODELISATION DE LA TURBULENCE.

Résumé :

Ce rapport décrit les techniques utilisées pour la mise au point d'un code de calcul permettant de simuler des écoulements compressibles. Les équations de Navier-Stokes compressibles, instationnaires, bidimensionnelles sont résolues via une approche différences finies en temps et éléments finis en espace. Une méthode de filtrage est utilisée sur les gradients des termes de convection pour assurer la stabilité du schéma numérique. Deux modèles de turbulence sont intégrés pour comparer et éventuellement améliorer les performances du modèle.

On présente des résultats numériques pour les écoulements autour d'un NACA0012 et d'une version simplifiée de la navette spatiale Hermès.

Notations :

Letters :

R^I : incompressible Reynolds stress tensor
R : compressible Reynolds stress tensor
τ : viscous and pressure stress tensor
σ : viscous stress tensor
S : strain tensor
μ_l : laminar viscosity
μ_t : turbulent viscosity
μ_r : reference viscosity
k : turbulent kinetic energy
q : square root of k
ϵ : turbulent dissipation rate
ω : defined by ϵ/k
α : inverse of the time step.

Non-letter symbols :

Γ, Γ_B, Γ_∞^+, Γ_∞^- : overall, body, downstream, upstream boundaries
Ω : computational domain
$\tilde{}$: mass-weighted averaging operator
$\hat{}$: value at the preceeding time step.
$\otimes$: tensor product $[(u \otimes u)_{ij} = u_i u_j]$

Spaces :

$L^2(\Omega)$: space of square Lebesgue integrable function.
$H^1(\Omega)$: usual Sobolev space of functions of $L^2(\Omega)$ whose first derivatives are also in $L^2(\Omega)$.
$X(\Omega) = \{x \in H^1(\Omega) | x_{|\Gamma \setminus \Gamma_\infty^+} = 0\}$
$Y(\Omega) = \{x \in H^1(\Omega) | x_{|\Gamma_\infty^-} = 0\}$

Remark: When needed, we use the classical tensor notation and the associated convention for repeated indices and derivatives.

Introduction

Numerical simulations of flows around airplanes and space vehicules at high Mach and Reynolds numbers are still a challenge to the numerical analyst. Most of the difficulties are taking their roots in the presence at the same time in the flow of complex physical phenomena of very different scales. The most frequently encountered are: shocks, boundary layers (both laminar and turbulent), wakes, and various interactions between these phenomena.

Throughout this paper, we make the hypothesis that all these phenomena are adequately modelized by the compressible Navier-Stokes equations. In particular, we suppose these equations valid for highly turbulent flows.

Under this hypothesis, our main problem is: how to solve the Navier-Stokes equations without over-damping some of these phenomena? The strategy of resolution presented is a step in that direction and is based on the following key ideas:

- first, being unable to represent the smaller physical scales, we take account of them throught a viscosity computed with appropriate turbulence models,
- second, unresolved frequencies following a shocks have to be damped by a numerical viscosity taking into account the physical viscosity,
- third, no a priori information about the boundary layer being reliable, we seek to resolve it directly, or eventually, by the use of special elements.

Altough very appealing, no wall law is used because even if the region where viscous effects are important is small, his influence is felt everywhere in the flow.

The formulation, schemes and method of solution where also chosen to meet some particular goals. In fact, it is our opinion that a good 2D Navier-Stokes code should include the following features :

(i) to be directly generalizable to 3D case,
(ii) to include a turbulent closure model with transport equations,
(iii) to be independent from the mesh,
(iv) to enable control of the numerical diffusion,
(v) to have solid theoretical support.

In this report, we present a resolution algorithm which includes most of these features ; (i), (iii) and (v) through a finite element approach, (ii) and (iv) through adequate use of classical methods.

The results of numerical experiments will be presented in order to show the possibilities of the methods discussed in this report.

1. Formulation of the Navier-Stokes equations for high Reynolds flows.

It is well-known (Matsumara-Nishida [1]) that with small initial data, the Navier-Stokes equations possess a unique solution. But in the usual case of large and stiff initial data, instabilities appear and degenerate in turbulence. We make the usual assumption that these cahotic flows are within the range of validity of the Navier-Stokes equations (albeit not within the capabilities of our numerical approximation of these equations).

Let $\Omega \in R^N$, (N=2 or 3 in practice), be the flow domain and Γ be its boundary. The conservative form of the equations is given below by :

$$\frac{\partial \rho}{\partial t} + \nabla \cdot (\rho u) = 0 \tag{1.1}$$

$$\frac{\partial \rho u}{\partial t} + \nabla \cdot (\rho u \otimes u) = \nabla \cdot (\tau), \quad \tau_{ij} = \tau_{ji} \tag{1.2}$$

$$\frac{\partial \rho E}{\partial t} + \nabla \cdot (\rho E u) = \nabla \cdot [\tau \cdot u - q] \tag{1.3}$$

$$\tau_{ij} = -p\delta_{ij} + \lambda S_{kk}(u)\delta_{ij} + 2\mu S_{ij}(u) \tag{1.4}$$

$$p = (\gamma - 1)\rho e \tag{1.5}$$

where, $S_{ij}(u) = \frac{1}{2}(u_{i,j} + u_{j,i})$, $E = e + \frac{1}{2}u^2$, $e = C_v T$, $\gamma = \frac{C_p}{C_v}$, $q = -k\nabla T$, $\lambda = -\frac{2}{3}\mu$.

In spite of all the recent advances in computer technology, turbulent flows cannot at present be computed by the direct resolution of the Navier-Stokes equations. The reason is that the turbulent motion contains a continuous range of scales in which the ratio of the larger to the smaller scale is about $0(Re^{3/4})$.

For this reason, and because one is generally not interested in complete details of the behavior of all the instantaneous variables, we work with the mass-weighted averages of those quantities.

To make it clear, we recall the definition of the averaging operators. If ρ is the instantaneous density and u the instantaneous velocity, then we define the average of ρ and the mass-average of u on a time interval of length t_0 by

$$\bar{\rho} = \frac{1}{t_0}\int_0^{t_0} \rho dt \ , \quad \tilde{u} = \frac{1}{\bar{\rho} t_0}\int_0^{t_0} \rho u dt$$

and u' by $u' = u - \tilde{u}$.

In order to simplify the writing, we will conserve the same notation for the mean variables and use the prime for the fluctuating part of mass-weighted variables. Consequently, for the remaining of the paper we set

ρ, p - mean density and pressure
u, e, T - mass-weighted mean velocity, internal energy and temperature
u', T' - fluctuating part of the velocity and the temperature
$\tilde{}$ - mass-weighted averaging operator.

Now, neglecting buoyancy effects and neglecting all viscosity and thermal conductivity fluctuations, the **open** equations for mass, momentum and total energy conservations are

$$\frac{\partial \rho}{\partial t} + \nabla \cdot (\rho u) = 0 \tag{1.6}$$

$$\frac{\partial \rho u}{\partial t} + \nabla \cdot (\rho u \otimes u) = \nabla \cdot [(\tau - (\rho \widetilde{u' \otimes u'}))] \tag{1.7}$$

$$\frac{\partial \rho E}{\partial t} + \nabla \cdot (\rho E u) = \nabla \cdot [(\tau - (\rho \widetilde{u' \otimes u'})) \cdot u - q_{tot}] \tag{1.8}$$

where $\rho E = \rho e + \frac{1}{2}\rho u^2 + \frac{1}{2}\rho \widetilde{u'^2} = \rho e + \frac{1}{2}\rho u^2 + \rho k$, k being the turbulent kinetic energy and q_{tot} the total (laminar + turbulent) heat transfert.

The system (1.6)-(1.8) contains only second order moments as supplementary unknowns, higher order moments being neglected and correlation between velocity and temperature modeled by $q_{i,tot} = -\lambda \frac{\partial T}{\partial x_i} + \widetilde{u_i' T'} = -\lambda_{tot} \frac{\partial T}{\partial x_i}$.

There are two ways to express the Reynolds stress tensor $R = -\rho \widetilde{u' \otimes u'}$:

•To assume that the Reynolds stresses are a local property of the mean flow and, by analogy with the viscous stresses, express them by a constitutive law.

•To assume that the Reynolds stresses are independant variable quantities and obtain their values through the resolution of a set of transport equations.

In this report, we consider only the first approach, the second requiring too much empirism (Rodi [1]).

The choice of a constitutive law relating R to mean quantities is very difficult. But, under certain approximations, Chacon-Pironneau [1], make it clear that, in the incompressible case, R^I and $(\nabla u + \nabla u^t)$ generate the same subspace of second-order tensors; hence in 2D

$$R^I = \alpha I + \beta(\nabla u + \nabla u^t) \tag{1.9}$$

where α, β are only functions of the nontrivial invariants of $(\nabla u + \nabla u^t)$, and possibly of the turbulent kinetic energy and a mixing length. We suppose that this can be generalized to the compressible case in the following way

$$R = -\rho \widetilde{u' \otimes u'} = -\frac{2}{3}(\rho k + \mu_t \nabla \cdot u)I + \mu_t(\nabla u + \nabla u^t) \tag{1.10}$$

More general hypotheses (Speziale [1]) seem to give more realistic approximations, but without any proof that the Reynolds stress tensor still lies in the same space of tensors.

In a classical way, we completely decouple the resolution of the mean Navier-Stokes equations (1.6)-(1.8) and the calculation of the Reynolds stresses.

The next section will be devoted to the resolution of the mean Navier-Stokes equations and section 3 to the modelization and the resolution of the model giving the Reynolds stresses.

2. Resolution of the Navier-Stokes equations for the mean flow.

We now consider the following non-conservative non-dimensional form of the Navier-Stokes equations (1.6)-(1.8). Details of the passage from the general equations to this system are included in the appendix 1.

$$\frac{\partial \rho}{\partial t} + u \cdot \nabla \rho + \rho \nabla \cdot u = 0 \tag{2.1}$$

$$\frac{\partial u}{\partial t} + (u \cdot \nabla)u + \frac{1}{\rho}\nabla\theta - \frac{1}{\rho}\nabla \cdot (\nu^* \sigma) = 0 \tag{2.2}$$

$$\frac{\partial T}{\partial t} + u \cdot \nabla T + \frac{\theta}{\rho}\nabla \cdot u - \nabla u : (\frac{\nu^*}{\rho}\sigma) - \frac{1}{\rho}\nabla \cdot (\kappa^* \nabla T) = 0 \tag{2.3}$$

in (2.1)-(2.3), we have normalized by the subscript r

(i) the density ρ by ρ_r
(ii) the velocity u by $|u_r|$
(iii) the internal energy e by $|u_r|^2$
(iv) the pressure p by $\rho_r |u_r|^2$
(v) the viscosities μ and μ_t by μ_r
(vi) the kinetic turbulence energy k by $|u_r|^2$
(vii) the temperature T by $|u_r|^2/C_v$

which imply $e = T$.

The pressure obeys the ideal gas law, the number γ and the functions σ, θ, ν^*, κ^* are defined by:

- $\sigma = \nabla u + \nabla u^t - \frac{2}{3}\nabla \cdot uI$,
- $\theta = p + \frac{2}{3}\rho k$, $(p = (\gamma - 1)\rho T)$,
- $\gamma = C_p/C_v$ is the ratio of specific heats ($\gamma \cong 1.4$ in air).
- $\nu^* = (\mu + \mu_t)/Re_r$ is the total viscosity defined from the computed laminar and turbulent viscosities, divided by the reference Reynolds number $Re_r = \rho_r u_r L_r/\mu_r$.

• $\kappa^* = \gamma/Re_r(\mu/Pr + \mu_t/Pr_t)$ is the total conductivity coefficient, also define from laminar and turbulent viscosities.
Remark: The field $(\nu^*)^{-1}$ will be referenced as the total Reynolds number field.

We consider external flows around 2D geometries; the domain of computation is described in figure 1a. Let Γ_∞ be a far-field boundary of the domain; we introduce

$$\Gamma_\infty^- = \{x | x \in \Gamma_\infty, u_\infty . n < 0\}, \qquad \Gamma_\infty^+ = \Gamma_\infty \backslash \Gamma_\infty^-$$

where u_∞ denotes the free stream velocity and n the unit vector of the outward normal to Γ.

We assume the flow to be uniform at infinity, and the corresponding variables to be normalized by the free stream values; then for example, we prescribe at infinity

$u = u_\infty = \binom{cos\alpha}{sin\alpha}$, α is the angle of attack,
$\rho = 1$,
$T = T_\infty = 1/[\gamma(\gamma - 1)M_\infty^2]$,

where M_∞ denotes the free stream mach number.

The boundary conditions on the computational boundary Γ_∞ are:

on Γ_∞^- : $u = u_\infty$, $T = T_\infty$, $\rho = 1$,
and on Γ_∞^+ : $\nabla T \cdot n = 0$, $[n \cdot (\nabla u + \nabla u^t - \frac{2}{3}\nabla \cdot uI) \cdot n] = 0$, $[n \cdot (\nabla u + \nabla u^t - \frac{2}{3}\nabla \cdot uI) \cdot t] = 0$,
where n, t, are the local normal and tangent on Γ_∞^+.

On the rigid boundary Γ_B, we shall use the following conditions:

$u = 0$ (no-slip condition),
$T = T_B = T_\infty(1 + (\gamma - 1)/2M_\infty^2)$ (free stream total temperature).

Finally, since steady solutions are sought through time dependent equations, initial conditions have to be added; we shall take
$\rho(x, 0) = \rho_o(x)$, $u(x, 0) = u_o(x)$, $T(x, 0) = T_o(x)$.

Solving the compressible Navier-Stokes equations is a difficult task. Most of the existing numerical solution methods are based on finite differences techniques, for both space and time discretizations. Following the work of Bristeau et al. [1][2], we will consider a method based on finite element techniques for space discretization while using finite differences in time.

Let the time derivatives be discretized using a classical implicit Euler finite differences formula, then at each time step, we solve the following non-linear system of variational equations

$$\alpha(\rho - \hat{\rho}, N) + (u \cdot \nabla\rho, N) + (\rho\nabla \cdot u, N) = 0 \tag{2.4}$$

$$\alpha(u - \hat{u}, M) + ((u \cdot \nabla)u, M) + (\frac{1}{\rho}\nabla\theta, M) + (\frac{\hat{\nu}^*}{\rho}\sigma, \nabla M) = 0 \tag{2.5}$$

$$\alpha(T - \hat{T}, K) + (u \cdot \nabla T, K) + (\frac{\theta}{\rho}\nabla \cdot u, K) - (\nabla u : (\frac{\hat{\nu}^*}{\rho}\sigma), K) + (\frac{\hat{\kappa}^*}{\rho}\nabla T, \nabla K) = 0 \tag{2.6}$$

where the solution is looked for in V x W x Z,

$$V = \{\rho \in H^1(\Omega) | \rho_{|\Gamma_\infty^-} = 1\}$$

$$W = \{u \in (H^1(\Omega))^2 | u_{|\Gamma_\infty^-} = u_\infty, u_{|\Gamma_B} = 0\}$$

$$Z = \{T \in H^1(\Omega) | T_{|\Gamma_\infty^-} = T_\infty, T_{|\Gamma_B} = T_B\}$$

although there is no complete theoretical justification of this. We look for a triple $(\rho, u, T) \in V$ x W x Z such that (2.4)-(2.6) is verify for all triple of test functions $(N, M, K) \in Y(\Omega)$ x $(X(\Omega))^2$ x $X(\Omega)$. For the definition of the spaces $X(\Omega)$, $Y(\Omega)$ see the page about notation.

Remark 1.: (,) denotes the scalar product in $L^2(\Omega)$.
Remark 2.: The natural boundary condition already defined, were introduced by setting the boundary integrals appearing from the integration by part to zero.
Remark 3.: The θ term of equation (2.5) is integrated in the form

$$\frac{1}{\rho}\nabla\theta = (\gamma - 1)\nabla T + \frac{4}{3}q\nabla q + [(\gamma - 1)\frac{T}{\rho} + \frac{2}{3}\frac{q^2}{\rho}]\nabla\rho$$

We do not integrate by part the pressure term of the momentum equation because we cannot set $p + \sigma_{nn} = 0$ on the boundary (doing so would perturbate the solution) and we prefer to avoid the computation of boundary integrals.

To approximate (2.4)-(2.6), by the finite element method, we must divide Ω into small elements (triangles) and replace all the functions by their interpolate ρ_h, u_h, T_h. Interpolates are defined inside the elements from their values at the nodes of the elements by an interpolation formula.

The choice of the approximation spaces is a critical and still partly obscur point. But, we see that when u is very small, for example near a solid boundary, equation (2.4) looks like a divergence free equation. This is specially true after the change of variable: $\sigma = \log\rho$ (see Bristeau et al. [1]). We may conjuncture that to ensure stability, a necessary condition is that the element chosen should be stable for the incompressible case. This seem to be confirmed by the various experiments made by Bristeau et al. [2].

A possible choice of such an element (and consequently spaces) is the $P_1 - iso\ P_2$ element (figure 1b). If $T_{h/2}$ is the triangulation obtained from T_h by dividing each triangle of T_h into 4 equal triangles whose vertices are the vertices $\{q^1, q^2, q^3\}$ of T_h and $\{\frac{1}{2}(q^1 + q^2), \frac{1}{2}(q^2 + q^3), \frac{1}{2}(q^1 + q^3)\}$, we define

$$V_h = \{\rho_h \in V | \rho_h \in C^o(\Omega), \forall T \in T_h, \rho_{h|T} \in P^1(T)\} \subset V$$
$$W_h = \{u_h \in W | u_h \in (C^o(\Omega))^2, \forall T \in T_{h/2}, u_{h|T} \in P^1(T)\} \subset W$$
$$Z_h = \{T_h \in Z | T_h \in C^o(\Omega), \forall T \in T_h, T_{h|T} \in P^1(T)\} \subset Z$$

where $P^1(T) = \{$ set of polynomials of degree ≤ 1 on $T\}$.

Restricted to these finite dimensional spaces, equations (2.4)-(2.6) lead to the non-linear problem:

Find (ρ_h, u_h, T_h) in $(V_h$ x W_h x $Z_h)$ solution of $F_h(\rho_h, u_h, T_h) = 0$, (2.7)

F_h being the discrete version (see appendix 2) of the system (2.4)-(2.6).

We now consider iteration schemes for solving the nonlinear system $F_h(s) = 0$, where $s = (\rho_h, u_h, T_h)$.

Newton's method applied to this system results in the iteration

1. Set s^o an initial guess
2. For n = 0,1,2,... until convergence do:
   2.1 Solve $J(s^n)\delta^n = -F_h(s^n)$, (2.8)
   2.2 Set $s^{n+1} = s^n + \delta^n$,

where $J(s^n) = F'(s^n)$ is the system Jacobian. For large problems, iterative methods are frequently used to solve (2.8) only approximately, giving rise to methods which can be viewed as inexact Newton methods. The particular method we use is the Generalized Minimum Residual Method (GMRES) due to Saad and Schultz [1]. This method has the virtue of requiring virtually no matrix storage and requires only the action of the Jacobian matrix J times a vector r, and not J explicitly. In the setting of nonlinear equations, this action is approximated by a difference quotient of the form

$$J(s)r \cong \frac{F_h(s+br) - F_h(s)}{b}$$

where s is the current approximation of a root of (2.7) and b is a scalar. For details of the algorithm, see Saad-Schultz [1] and also Bristeau et al. [2] for a clear setting of this algorithm within the context of the conjugate gradient methods.

To conclude this section we present and discuss two strategies to add some numerical diffusion in the approximation of the convective part of the equations.

It is well known that when the Reynolds number is high, boundary layers and shocks become hard to resolve and centered approximation of first derivatives are dangerous. In fact, it is necessary to add some numerical diffusion where the meshsize h is such that the local Peclet number satisfies the condition

$$Pe = \frac{ah}{\epsilon} > 2, \quad a = \rho \max(|u_1|, |u_2|),$$

in order to damp unresolved frequencies. There are many different ways to do that, upwinding, addition of an artificial viscosity,... but the problem is to control the numerical diffusion to be sure it does not degenerate the approximation of gradients.

Our approach is to filter the discrete gradients in the following way: as the discrete gradients are constant by element, we define the gradients at a node or on an element by an upwinded combination of the gradients on the nearby elements.

The first method can be viewed as a projection followed by a combination with the upwinded gradients. That is, if a node s is surrounded by elements 1 to n, with respective area a_k which sum to A. Then we define the gradient of a function ϕ at s by the combination of a centered gradient and an upwinded gradient

$$\nabla\phi_s = (1-\beta)\nabla\phi_s^c + \beta\nabla\phi_s^u \ , \tag{2.9}$$

where the centered and upwinded gradients at s are respectively defined by

$$\nabla\phi_s^c = \frac{1}{A}\sum_{k=1}^{n} a_k \nabla\phi_k \ , \quad \nabla\phi_s^u = \nabla\phi_{T(s)} \ ,$$

where $T(s)$ is the upwind element at node s. The choice of β will be discussed below.

The second method is a pure filtering and can also be written as a combination of a centered and an upwinded gradient. More precisely on an element e we define the gradient by

$$\nabla\phi_e = (1-\beta)\nabla\phi_e^c + \beta\nabla\phi_e^u \ , \tag{2.10}$$

where the centered and upwinded gradients on e are respectively defined by

$$\nabla\phi_e^c = \nabla\phi \ , \quad \nabla\phi_e^u = \frac{1}{3}\sum_{i=1}^{3} \nabla\phi_{T(s_i)} \ .$$

A fondamental difference between these two upwinding methods (for elements where gradients are constant by element) is that in the second there is no need for projection.

We now describe the computation of β. The method, based on the analysis of the scalar steady convection diffusion equation, is to relate the coefficient to a local Peclet number by:

$$\beta = \coth(\frac{Pe}{2}) - \frac{2}{Pe} ,$$

where the Peclet number is an estimation of the importance of convection compared to diffusion. Although the definition of this number is obvious in the scalar case, the generalization to multi dimensional cases is not immadiate. But in general we may define it by

$$Pe = Re\rho\hat{h}\hat{a} ,$$

where $\hat{h}$ is an estimation of the characteristic length and $\hat{a}$ an estimation of the convection speed.

A possible choice for $\hat{h}$, $\hat{a}$ is

$$\hat{h} = |(h \cdot u)|/|u| , \quad \hat{a} = |u| . \tag{2.11}$$

But some computational experiments demonstrated that the following choices, inspired from the work of Hughes et al. [1], give better results,

$$\hat{h} = |(h \cdot \nabla\phi)|/|\nabla\phi| , \quad \hat{a} = |(u \cdot \nabla\phi)|/|\nabla\phi| . \tag{2.12}$$

In fact, with these definitions, β is more closely related to discontinuities.

Note also that the coefficient β can be multiplied by a tuning coefficient for further control of the diffusion and more specifically to weight the diffusion added in each equation. The equation for ρ being the only equation without any physical diffusion it is fair to believe that more numerical diffusion should be added to this equation.

Altough less robust, the second method, the filtering method (2.9)-(2.12), proved to be very efficient and precise, provided that the mesh is adequately refined.

Remark: The value of $h = (h_x, h_y)$ at a given point of the mesh is deduced from the computed value on each element using the relations

$$|q_{1,x}| = \frac{a}{h_x}, |q_{2,x}| = \frac{1}{h_x}, |q_{2,x}| = \frac{(1-a)}{h_x}, \Rightarrow |q_{1,x}| + |q_{2,x}| + |q_{3,x}| = \frac{2}{h_x}$$

where q_i are the P_1 basis functions on a given triangle.

3. Closure model of turbulent flow.

The basic goal in developing turbulence models is to specify closure conditions in which the unknown Reynolds stresses of turbulence are related, either algebraically or through differential relations, to known mean-flow variables. The fundamental problem is to deduce a suitable mathematical model which should be a good compromise between mathematical simplicity and the complex exact transport equations of Reynolds stresses.

Our starting point will be the classical $k - \epsilon$ model of Jones-Launder [1]. A reason for it is that this model can be deduced rigorously in the incompressible case (Chacon-Pironneau [1]) and also because there is some efficient (but not trivial) ways to solve it.

It is well known (Huttar et al. [1]) that the choice of the scheme to solve the $k - \epsilon$ equations is very important. Thus, in order to ensure numerical stability we make a change of variable inspired by Coakley [1].

The basic closure turbulence model as described in the appendix 3 is given by

$$\frac{\partial(\rho q)}{\partial t} + u \cdot \nabla(\rho q) + \frac{1}{2}\rho q \nabla \cdot u - \frac{1}{2q} R : \nabla u + \frac{1}{2}\rho\omega q - \nabla \cdot [(\mu + \frac{\mu_t}{\sigma_q})\nabla q] = 0 \tag{3.1}$$

$$\frac{\partial(\rho\omega)}{\partial t} + u \cdot \nabla(\rho\omega) + \rho\omega\nabla \cdot u - (c_1 - 1)\frac{\omega}{q^2}R : \nabla u + (c_2 - 1)\rho\omega^2 - \nabla \cdot [(\mu + \frac{\mu_t}{\sigma_\omega})\nabla\omega] = 0 \qquad (3.2)$$

where $q^2 = k$, $\omega = \epsilon/k$, $\mu_t = c_\mu \rho q^2/\omega$ and R is the Reynolds stress tensor.

In the construction of two equations closure model it is assumed that the flow is fully turbulent, and that the Reynolds number is everywhere high. Thus, in order to provide predictions of the flow within the viscous layer adjacent to the wall, the above model must be extended in three ways. These are :

(i) prescribe the turbulent/non-turbulent interface,

(ii) the terms containing the c_1 and c_μ will become dependent upon the Reynolds number of turbulence,

(iii) if possible, correct values using empirical formulas.

The complex problem of the interface between a turbulent region and a non-turbulent region will not be discussed here.

The corrected values for the constants, proposed by Coakley [1], are given by replacing c_μ by $c_\mu D$ and $(1 - c_1)$ by $(0{,}405D + 0{,}045)$, where D is a damping factor given by

$$D = [1 - \exp^{-\alpha r}], \qquad r = \frac{\rho q^2}{\mu\omega}$$

where the value of the constant is $\alpha = 0.0018$.

Initial profiles for q and ω and corrected values are deduced from an estimation of the turbulent viscosity provided by an algebraic model, namely the Baldwin-Lomax [1] model, through the empirical relations

$$k = \frac{10}{3\rho}\mu_t S_{12} \quad \text{(Bradshaw hypothesis).}$$

$$\omega = \frac{3}{10}S_{12} \quad \text{(Hypothesis : production = dissipation).}$$

As in the case of the mean Navier-Stokes equations we work with the non-conservative (see appendix 4) and non-dimensional form of these equations. That is,

$$\frac{\partial q}{\partial t} + u \cdot \nabla q - \frac{1}{6}q\nabla \cdot u - \frac{q}{2\omega}c_\mu D(\sigma : \nabla u) + \frac{1}{2}\omega q - \frac{1}{\rho}\nabla \cdot [C_q \nabla q] = 0 \qquad (3.3)$$

$$\frac{\partial \omega}{\partial t} + u \cdot \nabla\omega + \frac{2}{3}(c_1 - 1)\omega\nabla \cdot u - (c_1 - 1)c_\mu D(\sigma : \nabla u) + (c_2 - 1)\omega^2 - \frac{1}{\rho}\nabla \cdot [C_\omega \nabla\omega] = 0 \qquad (3.4)$$

in (3.3)-(3.4), we have normalized by the subscript r

(i) ρ, u, T as in section 2

(ii) the viscosities μ and μ_t by μ_r

(iii) the kinetic turbulence energy q^2 by $|u_r|^2$

(iv) the specific dissipation rate of q^2, ω by $|u_r|/L_r$.

The functions D, σ, C_q, C_ω are defined by:

- $D = 1 - \exp(-\alpha\rho q^2 Re_r/\omega)$,
- $\sigma = \nabla u + \nabla u^t - \frac{2}{3}\nabla \cdot uI$,
- $C_q = (\mu + \mu_t/\sigma_q)/Re_r$,
- $C_\omega = (\mu + \mu_t/\sigma_\omega)/Re_r$,

The values of the constants c_μ, c_1, c_2, $\sigma_q = \sigma_k$ are taken from the original paper of Launder-Spalding [1], for the value of σ_ω see the appendix 3.

The boundary condition on smooth wall boundaries are $q = 0$ and $\nabla\omega \cdot n = 0$. At the computational boundary Γ_∞ small values are prescribed; $q = q_\infty$, $\omega = \omega_\infty$. More exactly, q_∞ is set to the known free stream value of the kinetic turbulent energy and ω_∞ is defined by setting

$$\mu_t = \frac{Re_r c_\mu \rho_\infty q_\infty^2}{\omega_\infty} = 1 .$$

We now describe the resolution strategy.

As already noted, the overall resolution is split in two parts; first we solve the mean Navier-Stokes equations then we solve the turbulence closure equations. At each step the resolution of (3.3)-(3.4) is done with $\rho = \hat{\rho}, u = \hat{u}, \mu = \hat{\mu}$, that is with known values from the preceeding Navier-Stokes step.

The technique used to solve (3.3)-(3.4) is very similar to that used, in section 2, to solve the mean Navier-Stokes equations and is based on the following weak formulation.

Let the time derivative be discretized using a classical implicit Euler finite differences formula, then at each step, we solve the following non-linear system of variational equations

$$\alpha(q - \hat{q}, N) + (\hat{u} \cdot \nabla q, N) - \frac{1}{6}(q\nabla \cdot \hat{u}, N) - (\frac{q}{2\omega} c_\mu D\hat{\sigma} : \nabla\hat{u}, N) + \frac{1}{2}(\omega q, N) + (\frac{\hat{C}_q}{\rho}\nabla q, \nabla N) = 0 \qquad (3.5)$$

$$\alpha(\omega - \hat{\omega}, K) + (\hat{u} \cdot \nabla\omega, K) + \frac{2}{3}(c_1 - 1)(\omega\nabla \cdot \hat{u}, K) - (c_1 - 1)(c_\mu D\hat{\sigma} : \nabla\hat{u}, K) + (c_2 - 1)(\omega^2, K) + (\frac{\hat{C}_\omega}{\rho}\nabla\omega, \nabla K) = 0 \qquad (3.6)$$

where the solution is looked for in Q x S,

$$Q = \{q \in H^1(\Omega) | q_{|\Gamma\infty} = q_\infty, q_{|\Gamma_B} = 0\}$$

$$S = \{\omega \in H^1(\Omega) | \omega_{|\Gamma\infty} = \omega_\infty\}$$

Here again, we obtain an approximation of the solution using the inexact Newton-GMRES method on the non-linear system (3.5)-(3.6) considered on the following finite dimensional approximation spaces,

$$Q_h = \{q_h \in Q | q_h \in C^o(\Omega), \forall T \in T_{h/2}, q_{h|T} \in P^1(T)\} \subset Q$$

$$S_h = \{\omega_h \in S | \omega_h \in C^o(\Omega), \forall T \in T_{h/2}, \omega_{h|T} \in P^1(T)\} \subset S$$

where $P^1(T) = \{$ set of polynomial of degree ≤ 1 on $T\}$ and $T_{h/2}$ is the fine grid of the $p_1 - iso\ p_2$ grids system discussed in section 2.

To make our scheme stable, we replace the convection terms $(\hat{u} \cdot \nabla q, N)$ and $(\hat{u} \cdot \nabla\omega, K)$ by filtered terms, (see section 2 for the filtering technique).

The second model of turbulence we use is an algebraic model derived from the Baldwin-Lomax [1] model. We include this model as a basis for comparison an eventually to decrease the cost of computation. (Another reason was to try to combine both models but preliminary computations lead us to the conclusion that the two equations model gives better results.)

In this model, the turbulent viscosity is computed using a two layer approach

$$\mu_t = \begin{cases} \mu_{ti}, & \text{if } Y \leq Y_c; \\ \mu_{to}, & \text{if } Y > Y_c. \end{cases}$$

where Y is the normal distance from the surface and Y_c is the least value of Y at which $\mu_{ti} = \mu_{to}$.

In the inner layer

$$\mu_{ti} = K^2 \rho |\omega| Y^2 [1 - exp(-Y^+/26)]^2$$

where ω is the vorticity, and $Y^+ = Y(\rho_o|\sigma_u|/\mu_o^2)^{1/2}$ with the subscript o referring to the value of the parameter at the nearest solid boundary and σ_u is the local shear stress in the direction of the flow.

In the outer layer

$$\mu_{to} = KC_{cp}\rho F_{\max} Y_{\max} F_{\text{kleb}} ,$$

where $F_{\max} = \max(Y|\omega|[1-\exp(-Y^+/26)])$, and $Y_{\max}$ is the value of Y at which $F_{\max}$ occurs. The Klebanoff intermittency correction is given by $F_{\text{kleb}} = [1 + 5,5(C_{\text{kleb}}Y/Y_{\max})^6]^{-1}$.

The model constants and functions are K = 0,40, k = 0,0168,

$$C_{cp} = \begin{cases} 0,2933 M_\infty + 1,2 , & \text{if } M_\infty < 3 ; \\ 2,08 , & \text{if } M_\infty \geq 3 , \end{cases}$$

$$C_{\text{kleb}} = \begin{cases} -0,4118 M_\infty + 0,65 , & \text{if } M_\infty < 0,85 ; \\ 0,3 , & \text{if } M_\infty \geq 0,85 . \end{cases}$$

In the wake region, the following non classical formulation is used

$$\mu_t = \mu_{tr}(|\omega|/|\omega_r|)$$

with the subscript r referring to a reference profile, usually the last profile before the trailing edge. This unusual wake formulation enable us to simulate the characteristic transport-diffusion behavior of the turbulence in the wake, keeping the emphasis on the evolution of the vorticity. This scheme avoids the appearence of steep gradients when moving from the wall model to the wake model of the usual algebraic models.

Some details about the implementation of this model for unstructured meshes are given in the appendix 5.

4. Resolution scheme.

We summarize here the overall resolution scheme as described in the previous sections. This reads :

Step 1: read initial values of u^o, ρ^o, T^o or let $\rho^o = 1$ and solve $\Delta u^o = 0$, $\Delta T^o = 0$ with appropriate boundary conditions.

Step 2: let $q^o = q_\infty, \omega^o = \omega_\infty, (q^o_{|\Gamma_B} = 0)$.

Step 3: $u^n, \rho^n, T^n, \mu_t^n, q^n, \omega^n$ being known from the previous time step

Step 3.1: update the laminar viscosity (μ^{n+1}) using the Sutherland formula,

Step 3.2: compute the algebraic viscosity ($\mu_{t,alg}^{n+1}$) using the Baldwin-Lomax model,

Step 3.3: make a correction to q^n and ω^n

$$q^{n+1/2} = \max[q^n, q_\infty] , \quad \omega^{n+1/2} = \max[\omega^n, \omega_\infty]$$

or

$$q^{n+1/2} = \max[(\frac{10\mu_{t,alg}^{n+1} S_{12}^n}{3\rho^n Re_r})^{1/2}, q^n, q_\infty]$$

$$\omega^{n+1/2} = \max[\frac{3}{10} S_{12}^n, \omega^n, \omega_\infty]$$

Step 3.4: solve the $q-\omega$ equations $F_{q\omega}(q^{n+1},\omega^{n+1})=0$ (see section 3),

Step 3.5: update the turbulent viscosity (this step may include a projection of q and ω to eliminate negative values)

$$\mu_t^{n+1}=c_\mu D(q^{n+1})^2/\omega^{n+1}$$

or

$$\mu_t^{n+1}=\max[c_\mu D(q^{n+1})^2/\omega^{n+1},\mu_{t,alg}^{n+1}]$$

Step 3.6: solve the N-S equations $F_{NS}(u^{n+1},\rho^{n+1},T^{n+1})=0$ (see section 2),

Step 4: if $|s^{n+1}-s^n|_{L^2(\Omega)}<\epsilon$, $s^n=(\rho^n,u^n,T^n)$,then stop, else go to step 3.

5. Numerical experiments

Before the exposition of the results of the numerical experiments let us recall that as ν^* is defined from the laminar and the turbulent viscosities, it is not a fluid property. This field is of first interest, more exactly we are interested in the field $1/\nu^*$ called the total Reynolds number.

Computations were performed for some flow condition around a NACA0012 airfoil and a simplified version of the Hermès space shuttle. In each case, the steady state solution was reached after 80 to 120 time steps depending on whether the initial flow field was uniform or a known flow field from a previous computation. Two test cases were chosen here for the computations, each case involving complex flow with shock waves.

The first series of numerical experiments concern a compressible viscous and turbulent flow around a NACA0012 airfoil. A part of the coarse mesh used is shown in figure 2a. We took here $M_\infty=0.85$, $Re=10^5$, $\gamma=1.4$, $Pr=0.72$, $Pr_t=0.9$ and a zero angle of attack.

We have shown on figure 3 the isomach contours (figure 3a) for a Navier-Stokes computation with the total Reynolds number field deduced from the Sutherland formula (figure 3b). The same problem was solved a second time but using the two-equations turbulence model, discussed in section 3, for the computation of the total Reynolds number field. See figure 4 for the isomach contours and the total Reynolds number field and figure 5 for the iso-k and iso-ω contours. Despite the problems caused by the coarse mesh in the wake, we note the presence of vortices in both computation. In the turbulent one, the boundary layer thicken abruptly but did not damp out the time-dependant nature of the schocks and the wake vortices.

It is clear that this flow is under the capabilities of the mesh we use. But it is interesting to see that most of the physical phenomena we attend to see are present. The obvious way to obtain better results is to refine the mesh in regions where steep gradients are present. This is only a matter of computer facilities, but we are now developing a strategy to obtain better results via the use of enriched finite elements is the corresponding areas.

The second series of numerical experiments concern a compressible viscous and turbulent flow around a simplified version of the Hermès space shuttle. A part of the coarse mesh used is shown in figure 2b. We took here $M_\infty=2.0$, $Re=10^4$, $\gamma=1.4$, $Pr=0.72$, $Pr_t=0.9$ and a zero angle of attack. Note that the length of the body is approximatively 0.14 of characteristic length.

We have shown on figure 6 the isomach contours (figure 6a) for a Navier-Stokes computation with the total Reynolds number field given by the Sutherland formula (figure 6b). The same problem was solved a second time using the two-equations turbulence model, see figure 7 for the iso-k and iso-ω contours, but all the characteristics of the flow remainded similar (see for example the comparison of the friction coefficients for the turbulent and non-turbulent computation shown on figure 9b). This is encouraging because at this low Reynolds number the flow should be mainly laminar. We have conducted a sensibility experiment on the values of the constant σ_ω of the ω equation. The new iso-k and iso-ω contours for the last $q-\omega$ computation

with $\sigma_\omega = 13.$ instead of 1.3 are shown in figure 8. Altough satisfactory for a very wide range of flow condition (Coakley [2]) preliminary results on simple nearly incompressible cases tend to indicate that this choice for σ_ω leads to overdiffused values for $k = q^2$ and ω. That is, the constant σ_ω is not universal.

Finally, a numerical experiment was conducted to compare the diffusion associated with the turbulence model used. The test case was the transonic flow around a NACA0012 airfoil at $M_\infty = 0.85$, $Re = 10^4$, $\gamma = 1.4$, $Pr = 0.72$, $Pr_t = 0.9$ and a zero angle of attack. Computed values of the friction coefficient are displayed on figure 9a. The navier-Stokes computation (inner curves) show a large separation zone while the use of the algebraic turbulence model gives no separation at all (outer curves). It is clear that the diffusion caused by this turbulence model is over estimated. The estimation given by the two-equations model (see middle curves on figure 9a) is more realistic.

Other aspects of these computation can be seen on figures 10, 11 and 12.

Figure 10 display the mach contours and details of the tail flow for the Navier-Stokes computation without any turbulence model.

Figure 11 and 12 displays the mach contours and eddy viscosity for the Navier-Stokes computation with the algebraic turbulence model and the two-equations turbulence model, respectively.

The choices made in step 3.3 and step 3.6 of the resolution scheme (see section 4) were proved to be less important than expected. In fact, the solution process described to solve the turbulence transport equations with the given boundary and flow condition converge without the need of the algebraic turbulence model. The latter may be used to start the $q - \omega$ computation from a given state, causing the steady state to be reached faster.

We present here some statistics in order to give an idea of the time used for these computations on a SUN3 workstation with a floating point accelerator (0.4 Mflops). For a computation on the 1883 nodes simplified Hermès space shuttle, it takes at each time step:

110 seconds to compute the turbulent viscosity with the algebraic model,

2300 seconds to compute the turbulent viscosity with the two-equations model, (complete resolution at each time step),

1100 to 2000 seconds to solve the Navier-Stokes equations.

6. Concluding remarks.

We have presented a numerical scheme to solve the compressible Navier-Stokes equations written in non conservative form with emphasis on the turbulence modeling. We have obtained good results for moderate Reynolds numbers using an approximation satisfying some "inf-sup" condition and using a filtering of the gradients of the convective terms. This filtering is dependent of the local direction of the fluid flow and of the local amount of physical viscosity. A particuliar form of the $k - \epsilon$ model was solved with standard boundary condition to obtain an estimation of the turbulent viscosity using the same techniques.

Further developement are needed to obtain accurate solution for higher Mach and Reynolds numbers where special care have to be taken to dont introduce too much numerical dissipation. In a recent future we have planed to compare computations on finer grids with experimental tests and make emphasis on filtering-upwinding methods and also on the resolution of the boundary layers.

Appendix 1 to 5

Appendix 1: Non-conservative mean Navier-Stokes equations.

We present here the passage from the conservative system (1.6)-(1.8) to the non-conservative system (2.1)-(2.3). Actually, only the dimensional form will be derived.

First we substitute (1.10) in (1.6)-(1.8) to find,

$$\frac{\partial \rho}{\partial t} + \nabla \cdot (\rho u) = 0 \tag{1}$$

$$\frac{\partial \rho u}{\partial t} + \nabla \cdot (\rho u \otimes u) - \nabla \cdot \sigma = 0 \tag{2}$$

$$\frac{\partial \rho E}{\partial t} + \nabla \cdot (\rho E u) + \nabla \cdot (u \cdot \sigma) + \nabla \cdot q = 0 \tag{3}$$

where $\sigma = \theta I - (\mu + \mu_t)S$ with S, θ defined by:

- $S = \nabla u + \nabla u^t$,
- $\theta = p + \frac{2}{3}\rho k + (\mu + \mu_t)\frac{2}{3}\nabla \cdot u$,

To put the equations (1)-(2) in non-conservative form, we use the identities:

$$\nabla \cdot (\rho u) = \rho \nabla \cdot u + u \cdot \nabla \rho,$$

$$\nabla \cdot (\rho u \otimes u) = (u \otimes u) \cdot \nabla \rho + \rho u \nabla \cdot u + \rho u \cdot \nabla u,$$

$$\frac{\partial \rho u}{\partial t} = \rho \frac{\partial u}{\partial t} - \rho u \nabla \cdot u - (u \otimes u) \cdot \nabla \rho,$$

from which we deduce

$$\frac{\partial \rho}{\partial t} + u \cdot \nabla \rho + \rho \nabla \cdot u = 0 \tag{4}$$

$$\rho \frac{\partial u}{\partial t} + \rho (u \cdot \nabla) u + \nabla \theta - \nabla \cdot ((\mu + \mu_t) S) = 0 \tag{5}$$

For the energy equation (3) we proceed as follow: first expand the left hand side,

$$\frac{\partial \rho E}{\partial t} + \nabla \cdot (\rho E u) = \frac{\partial \rho e}{\partial t} + \frac{1}{2}\frac{\partial \rho u^2}{\partial t} + \nabla \cdot ((\rho e + \frac{1}{2}\rho u^2) u),$$

splitting all these terms and using the mass equation we find

$$\frac{\partial \rho E}{\partial t} + \nabla \cdot (\rho E u) = \rho \frac{\partial e}{\partial t} + \rho u \cdot \nabla e + u \cdot (\rho \frac{\partial u}{\partial t} + \rho (u \cdot \nabla) u)$$

then using the momentum equation,

$$\frac{\partial \rho E}{\partial t} + \nabla \cdot (\rho E u) = \rho \frac{\partial e}{\partial t} + \rho u \cdot \nabla e - u \cdot \nabla \theta + u \cdot \nabla \cdot ((\mu + \mu_t) S). \tag{6}$$

But the RHS of the energy equation can by writen,

$$-\nabla \cdot (u \cdot \sigma) - \nabla \cdot q = -\nabla \cdot (\theta u) + \nabla ((\mu + \mu_t) u \cdot S) - \nabla \cdot q.$$

Combining this with equation (6), we find,

$$\rho\frac{\partial e}{\partial t} + \rho u \cdot \nabla e = u \cdot \nabla\theta - \nabla \cdot \theta u + \nabla((\mu + \mu_t)u \cdot S)$$

$$-u \cdot \nabla \cdot ((\mu + \mu_t)S) - \nabla \cdot q.$$

But using the following identities

$$\nabla \cdot (\alpha w) = \alpha \nabla \cdot w + w \cdot \nabla\alpha,$$

$$\nabla \cdot (w \cdot M) = \nabla w : M + w \cdot \nabla \cdot M,$$

with $\alpha = \theta$, $w = u$, and $M = (\mu + \mu_t)S$, we find,

$$\rho\frac{\partial e}{\partial t} + \rho u \cdot \nabla e + \theta \nabla \cdot u - \nabla u : ((\mu + \mu_t)S) + \nabla \cdot q = 0$$

The usual non-conservative form follows from this by the use of the relation: $\nabla \cdot q = -\gamma((\frac{\mu}{Pr} + \frac{\mu_t}{Pr_t})\nabla e)$. Note that, for convenience, the functions θ, σ and S were redefined.

Appendix 2: Integration.

The nonlinear discrete system of equations to be solved follows from the consideration of the variational system (2.4)-(2.6) on proper finite dimensional spaces. Exact definitions of these spaces and the corresponding test spaces follow from the choice of the finite element. Now remains the problem of the evaluation of the various term, that is, the choice of an integration strategy. Exact integration will be use for first order terms but approximation will be made for higher order terms.

The basic formula for the integration is the Simpson's formula

$$\int_T w dx = \frac{meas(T)}{3}\sum_{i=1}^{3} w(m_{iT}), \qquad \forall w \in P_2,$$

where m_{iT} are the midnodes of the triangle T. Thus, the integral of the product of $f \in P_1$ by the basis function λ_j on the same triangle will be given by

$$\int_T f\lambda_j dx = \frac{meas(T)}{12}\left(\sum_{i=1}^{3} f(M_{iT}) + f(M_{jT})\right), \qquad \forall f \in P_1,$$

where M_{iT} are the nodes of the triangle T. The same formula is used for the integration of the product of a function define on the $isoP_2$ grid times the basis function λ_j of the P_1 grid. In this case, the formula reads

$$\int_T f\lambda_j dx = \frac{meas(T)}{96}\left(\sum_{i=1}^{3} f(M_{iT}) + 5f(M_{jT}) + 10\sum_{i=1}^{3} f(m_{iT}) - 6f(m_{jT})\right), \qquad \forall f \in isoP_2,$$

where m_{iT} are midnodes and M_{iT} are the nodes of the triangle T. For simplicity, these formulas are also used for higher order terms.

Appendix 3: Two equations closure model.

We give here some details about the two equations closure model (3.1)-(3.2) we used.

Let us recall the simplest and certainly the most popular closure model, namely, the $k - \epsilon$ model where k is the turbulence energy and ϵ is its rate of dissipation. According to this prescription

$$\mu_t = c_\mu \rho k^2/\epsilon$$

$$\frac{\partial(\rho k)}{\partial t} + u\nabla(\rho k) = -\rho k \nabla \cdot u + R : \nabla u + \nabla \cdot [(\mu + \frac{\mu_t}{\sigma_k})\nabla k] - \rho\epsilon \tag{1}$$

$$\frac{\partial(\rho \epsilon)}{\partial t} + u\nabla(\rho \epsilon) = -\rho\epsilon \nabla \cdot u + c_1 \frac{\epsilon}{k} R : \nabla u + \nabla.[(\mu + \frac{\mu_t}{\sigma_\epsilon})\nabla \epsilon] - c_2 \rho \frac{\epsilon}{k} \tag{2}$$

where $c_\mu, \sigma_k, \sigma_\epsilon, c_1, c_2$ are model constants, usually set to the recommended standard values 0.09, 1.0, 1.3, 1.44 and 1.92 respectively.

It is well known that near a solid boundary (at the boundary we suppose $k = \epsilon = 0$) this model needs a low-Reynolds number dissipation term to balance molecular diffusion in the sublayer. In fact, letting y tend to 0, equation (1) becomes

$$\cdot \mu k_{,yy} = 0$$

which is incompatible with the experimental fact that $k \sim y^2$ in the sublayer.

Instead of adding empirical terms to correct it, we assume k to be constant in the diffusion term and make the following change of variable $k = q^2$, from which we deduce directly equation (3.1). Note that if we assume $q^2 = k \sim y^2$ we obtain the correct behavior of q when $y \to 0$.

Finally, in order to reduce the problems of numerical instabilities, we reduce the truncation errors due to quotients, using the change of variable $\omega = \epsilon/k$. But this has to be paid by supplementary hypotheses.

If we put $\omega = \epsilon/k$ in equation (2) and use the identity

$$k(\rho\omega)' = \epsilon\rho' + (\rho\epsilon)' - \omega(\rho k)'$$

we find the equation

$$\frac{\partial(\rho\omega)}{\partial t} = \omega\frac{\partial\rho}{\partial t} + \omega u \cdot \nabla\rho - u \cdot \nabla(\rho\omega) + \frac{(c_1 - 1)\omega}{q_2} R : \nabla u + D - (c_2 - 1)\rho\omega^2 \tag{3}$$

where the diffusion term reads

$$D = \nabla \cdot [(\mu + \frac{\mu_t}{\sigma_\epsilon})\nabla\epsilon] - \omega\nabla \cdot [(\mu + \frac{\mu_t}{\sigma_k})\nabla k] \tag{4}$$

Thus we need to assume $(\mu_t + \mu_t/\sigma_\epsilon) = (\mu + \mu_t/\sigma_k) = \text{cte}$ in order to write it in the simpler form

$$D = \nabla \cdot [(\mu + \frac{\mu_t}{\sigma_\omega})\nabla\omega] \tag{5}$$

where the recommended value for σ_ω (Coakley [1]) is 1.3. But, altough satisfactory for a very wide range of flow condition (Coakley [2]) preliminary results on simple nearly incompressible cases tend to indicate that this choice for σ_ω leads to overdiffused values for $k = q^2$ and ω.

The standard form for this equation follows from the use of the non-conservative mass balance equation.

Appendix 4: Non-conservative closure equations.

We begin by developing the production terms. As $R : \nabla u = q^2 G(\omega, u)$ with G independant of q, the production terms are of the form (respectively)

$$(\frac{1}{q} R : \nabla\hat{u}, N) = ([c_\mu D\rho\frac{q}{\omega}(\nabla u + \nabla u_T - \frac{2}{3}\nabla \cdot uI) - \frac{2}{3}\rho q I] : \nabla u, N),$$

$$(\frac{\omega}{q_2} R : \nabla\hat{u}, K) = ([c_\mu D\rho(\nabla u + \nabla u_T - \frac{2}{3}\nabla \cdot uI) - \frac{2}{3}\rho\omega I] : \nabla u, K).$$

Note that the equation for ω is a nonlinear equation **independent** of q. Replacing the relations in equation (3.1) and (3.2) respectively, and using the same standard tricks as in appendix 1 we obtain the non-conservative form for these equations.

Appendix 5: Implementation of the algebraic turbulence model.

The fact that this kind of model is one of the most widely used takes its roots in the ease of its implementation in finite differences codes. The basic property appearing here is the orthogonality between the meshes lines and the walls. This important property will have to be replaced by an abstract structure for general finite elements meshes.

The most obvious way is to compute all the model parameters on a second mesh ensuring the orthogonality property and to use an interpolation operator between the two meshes. This procedure can be difficult to implement for complex (2-D) geometries and inadequate in 3-D.

Another way to implement algebraic turbulence models for general meshes is to consider independantly each node. That is, keeping some simple geometric characteristics of each node in a table, for example the nearest point of each walls, the normal lines passing trougthout this node can be found and so all the model parameters evaluated. But as usual, the simplicity of this method has to be paid; the maximization of functionals along the normal lines can be very costly. Consequently, the complexity of the process have to be diminished by the use of approximate maximization techniques and eventually by restricting the process to adequately chosen nodes. These simplifications makes the overall process interesting.

Acknowledgments.

This work is partly supported by a contract from Avions Marcel Dassault - Bréget Aviation. We would like to thank specially M.O. Bristeau and also M. Fortin, R. Glowinski, O. Pironneau, B. Cardot, J. Periaux for fruitful discussions.

References

B.S. Baldwin and H. Lomax [1] : Thin layer approximation and algebraic model for separated turbulent flows, AIAA Paper 78-0257 (1978).

S. Boivin [1] : A numerical method for solving the compressible Navier-Stokes equations, to appear in IMPACT of Computing in Science and Engineering, Academic Press Boston, (1989).

M.O. Bristeau, R. Glowinski, J. Périaux [1] : Numerical methods for the Navier-Stokes equations. Application to the simulation of compressible and incompressible viscous flows, Computer Physics Reports 6, (1987).

M.O. Bristeau, R. Glowinski, B. Mantel, J. Périaux, G. Rogé [2] : Adaptative finite element methods for three dimensional compressible viscous flow simulation in aerospace engineering, in: 11th Inter. Conf. on Numer. Meth. in Fluid Dynamics, Springer-Verlag (to be published) (1988).

T. Chacon and O. Pironneau [1] : On the mathematical foundation of the $k-\epsilon$ model, in : Vistas in applied mathematics. A.V. Balakrishnan ed. Optimization Software inc. Springer (1986).

T.J. Coakley [1] : Turbulence modeling methods for the compressible Navier-Stokes equations, AIAA Paper 83-1693, (1983).

T.J. Coakley [2] : Numerical simulation of viscous transsonic airfoil flows, AIAA 87-0461, (1987).

B. Escande [1] : Modélisation de l'interaction onde de choc/couche limite turbulente. Comparaison calcul-expérience, Thèse Doctorat, Ecole Centrale de Lyon (1986).

U.C. Goldberg [1] : Separated flow treatment with a new turbulence model, AIAA J., v. 24, no 10, (1986).

T.J.R. Hughes, M. Mallet and A. Mizukami [1] : A new finite element formulation for computational fluid dynamics: II. Beyond SUPG in Computer Methods in Applied Mechanics and Engineering, (1985).

A.G. Hutton, R.M. Smith and S. Hickmott [1] : The computation of turbulent flows of industrial complexity by the finite element method - progress and prospects in Finite Element in Fluids - Volume 7, John Wiley and Sons Ltd., (1987).

W.P. Jones and B.E. Launder [1] : The prediction of laminarization with a two equations model of turbulence, Int. J. Heat Mass Transfer, Vol. 15, (1972).

B.E. Launder and D.B. Spalding [1] : The numerical computation of turbulent flows in Computer Methods in Applied Mechanics and Engineering, Vol. 3, (1974).

A. Matsumara and T. Nishida [1] : Initial boundary value problems for the equations of motion of general fluids, in : Computing Methods in Applied Sciences and Engineering, V. North-Holland, (1982).

W. Rodi [1] : Turbulence models and their application in hydraulics, Inter. Asso. Hydro. Research, The Netherlands.

Y. Saad and M.H. Schultz [1] : GMRES: A generalized minimal residual algorithm for solving nonsymmetric linear systems, SIAM J. Sci. Stat. Comp., 7 (1986).

C.S. Speziale [1] : On nonlinear $k-l$ and $k-\epsilon$ models of turbulence, J. Fluid Mech.. 178, (1987).

M. Tabata [1] : Finite element approximation corresponding to the upwind finite differencing, Mem. Numer. Math. Univ. Kyoto and Tokyo Y, (1977).

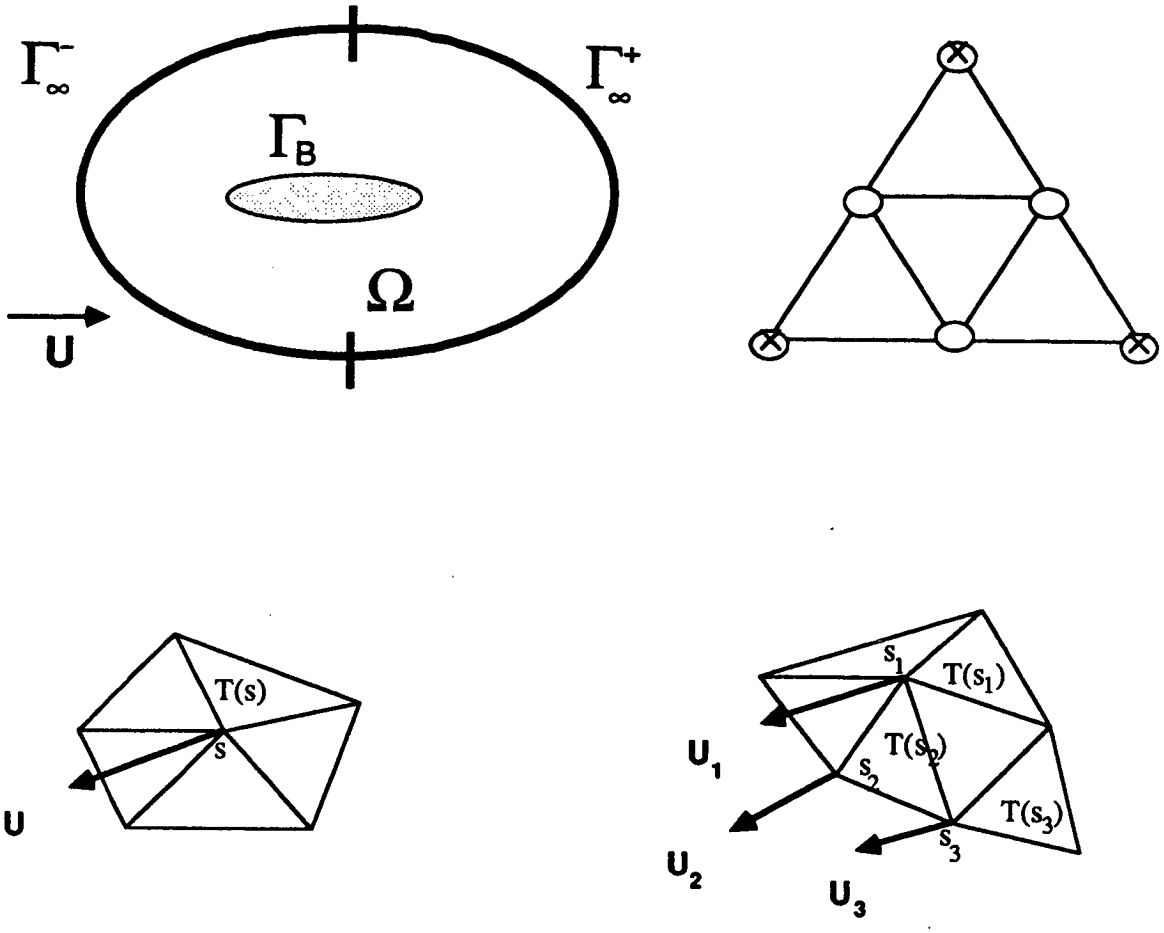

Figure 1: a) Computational domain,

b) P_1 - iso. P_2 element: ⊗ velocity, density, temperature, q and w d.o.f.,
○ velocity, q and w d.o.f.,

c) Upwind finite element T(s), to node s,

d) Upwind finite elements $T(s_i)$, to nodes s_i of a given element.

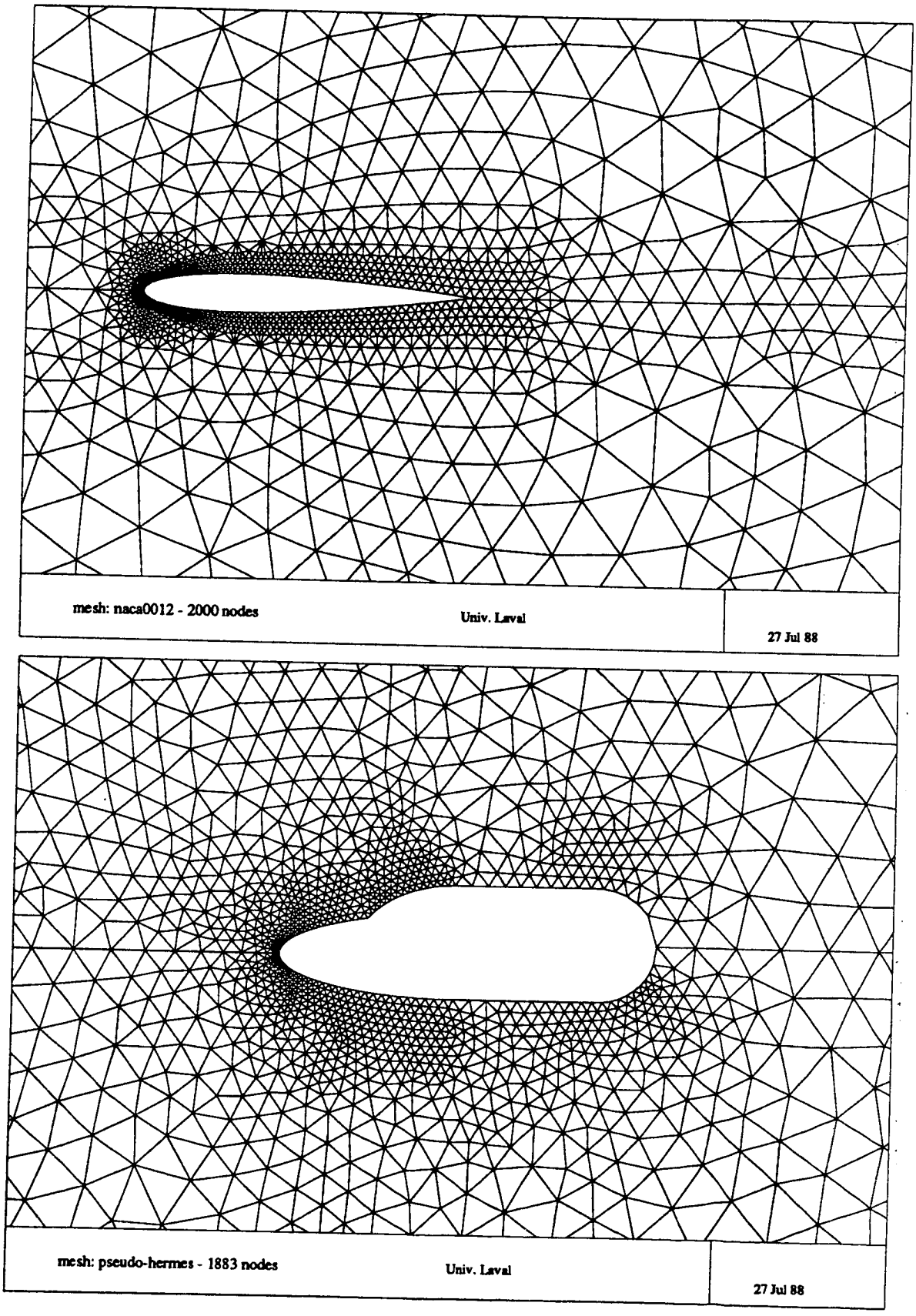

Figure 2: Partial view of the principal meshes.

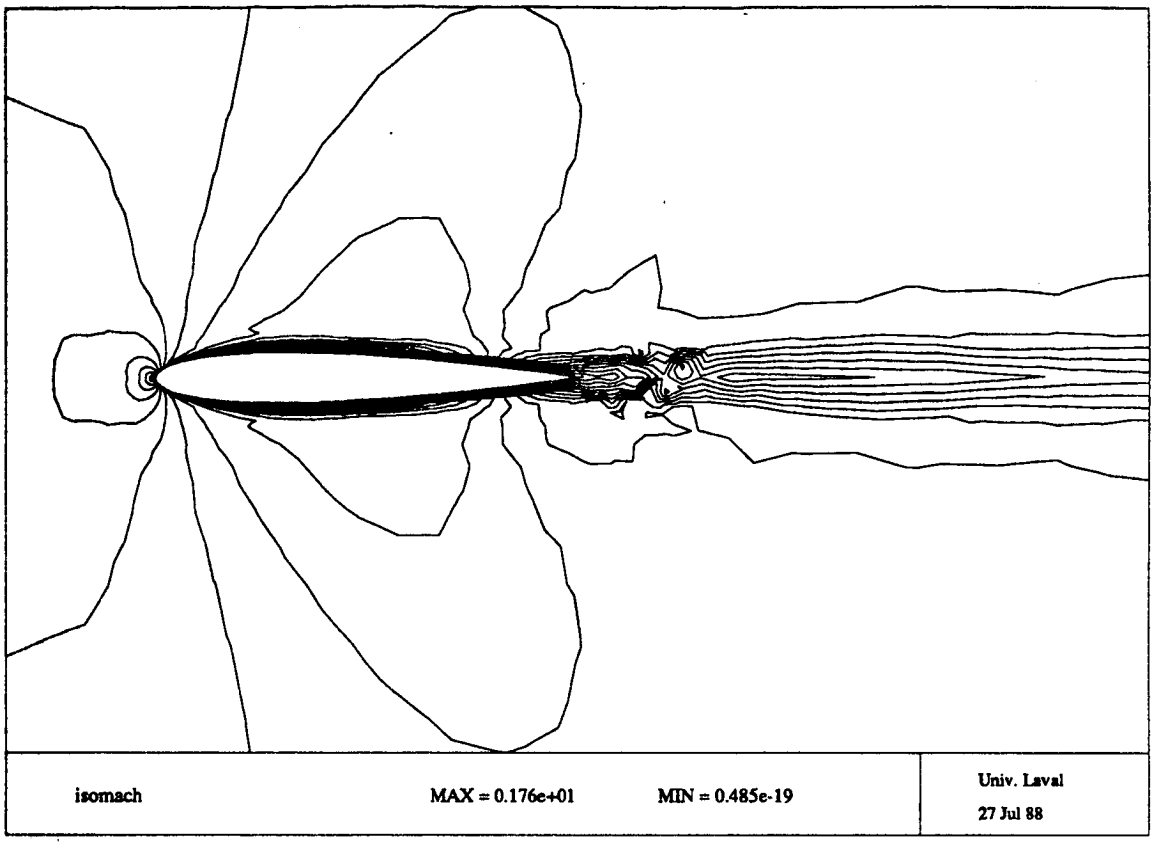

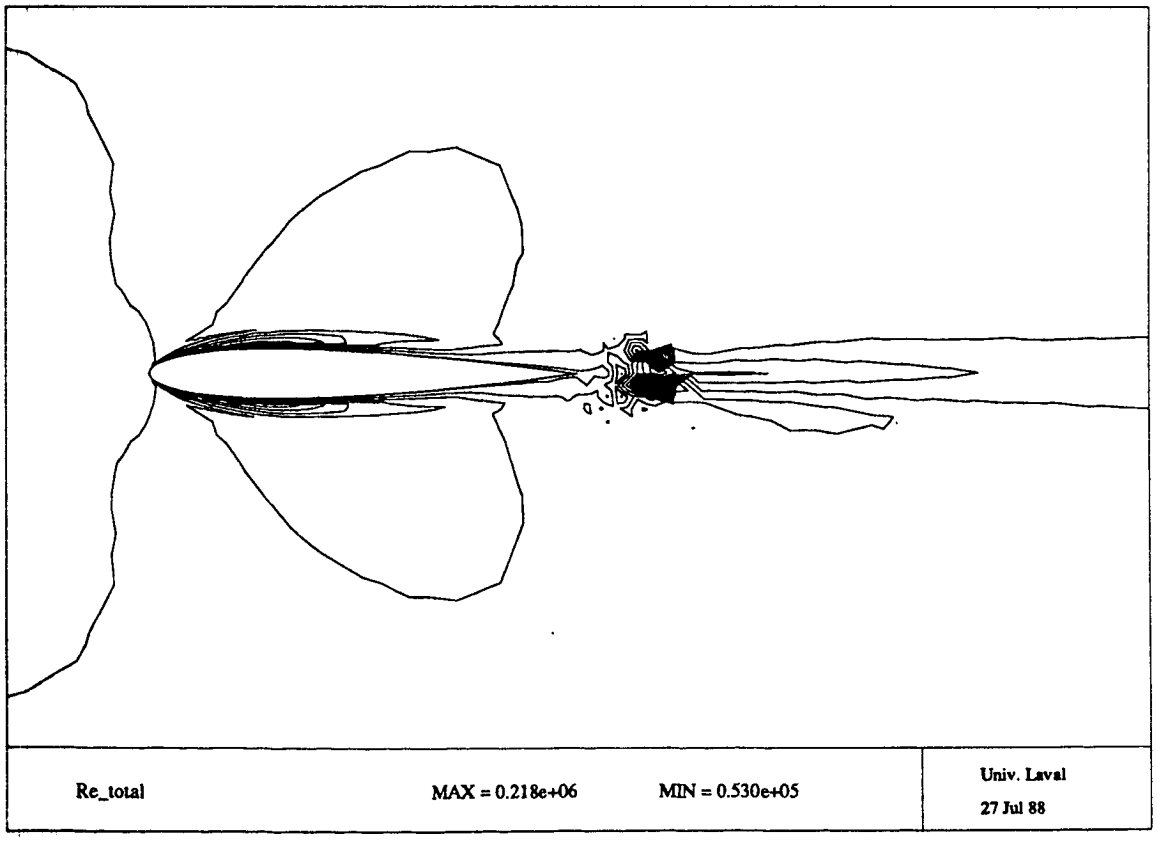

Figure 3: Mach contours and total Re number, laminar computation at M=.85, Re=10e5.

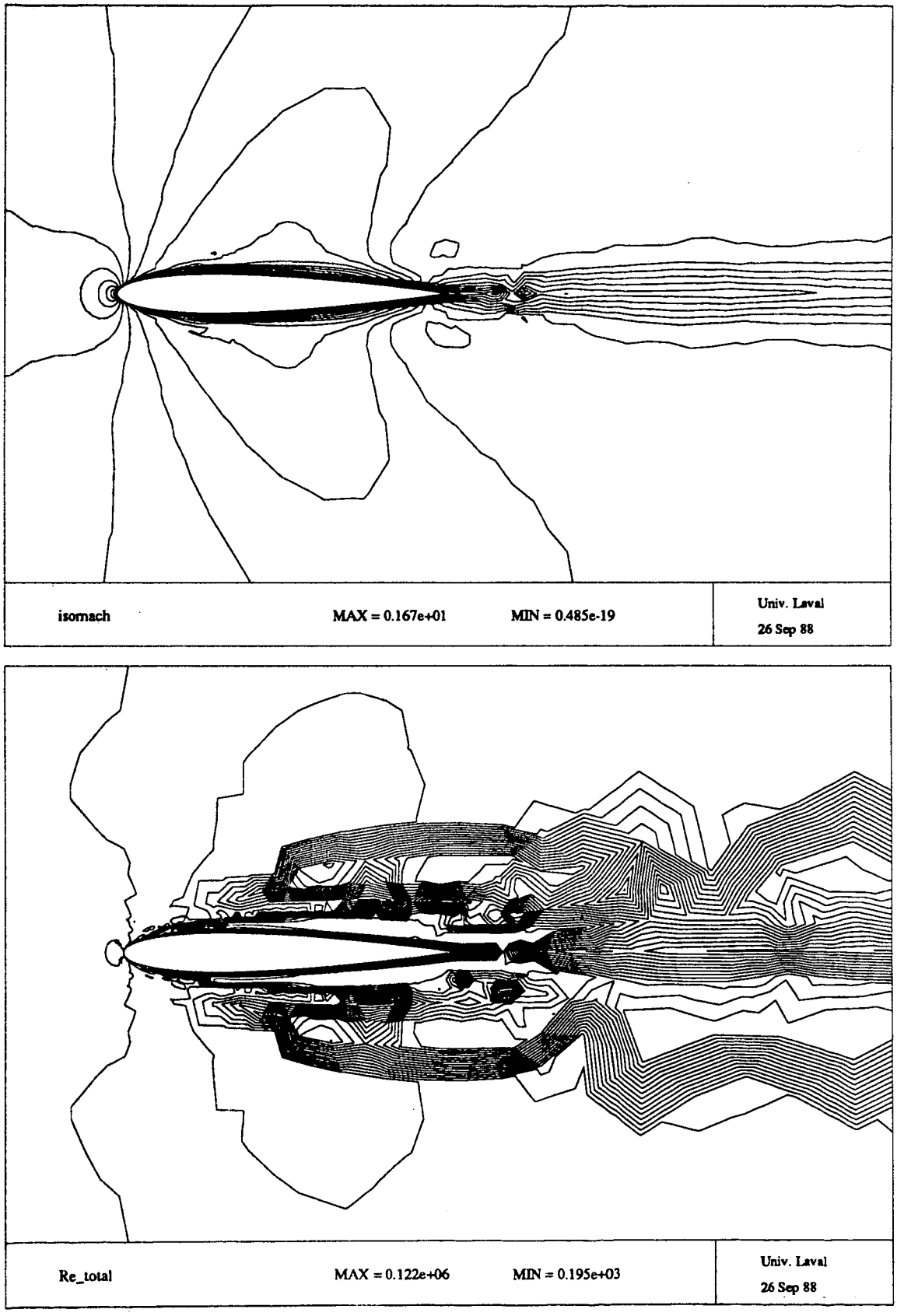

Figure 4: Mach contours and total Re number, q-w computation at M=.85, Re=10e5.

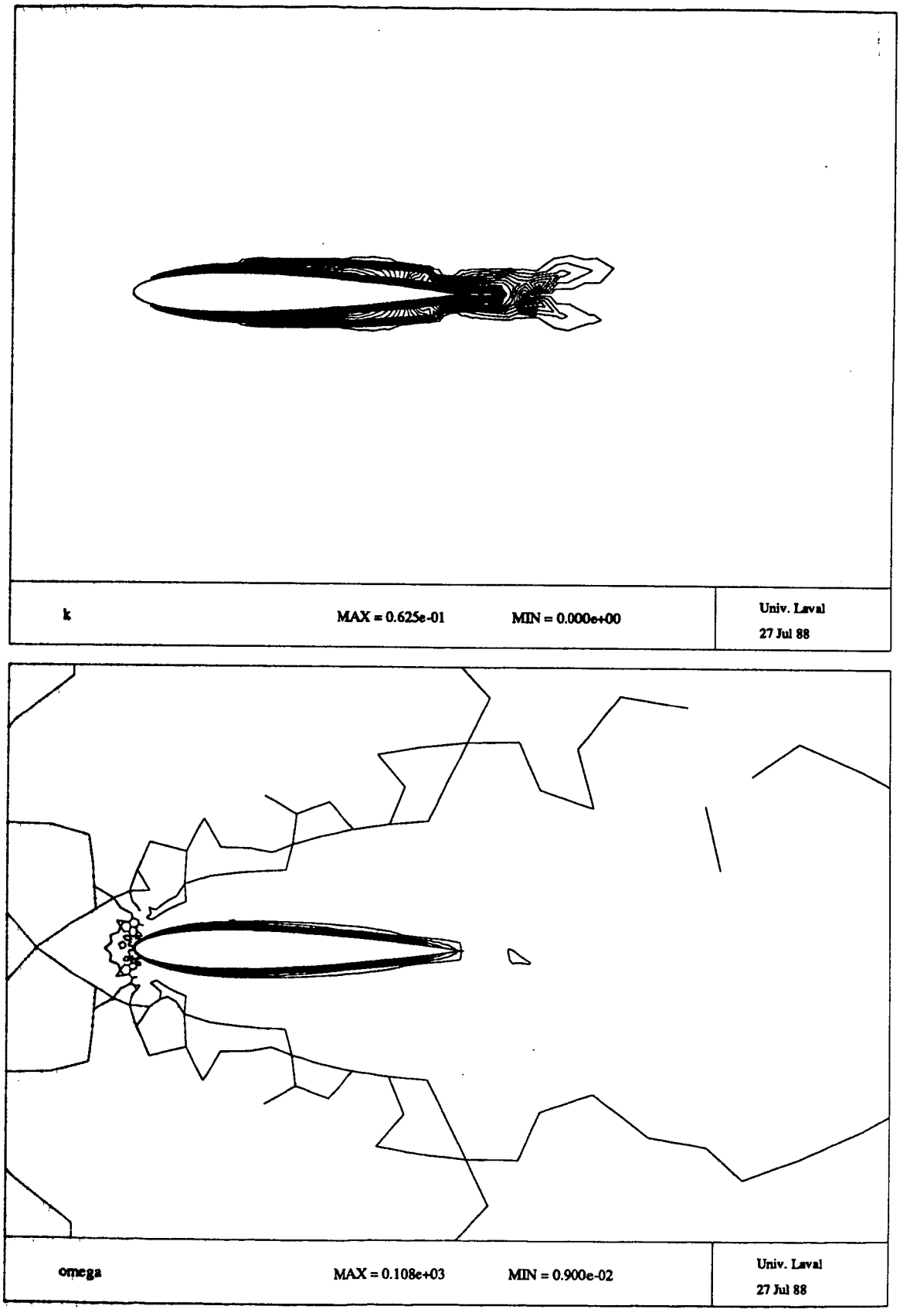

Figure 5; k and w from a q-w computation at M=0.85, re=10e5.

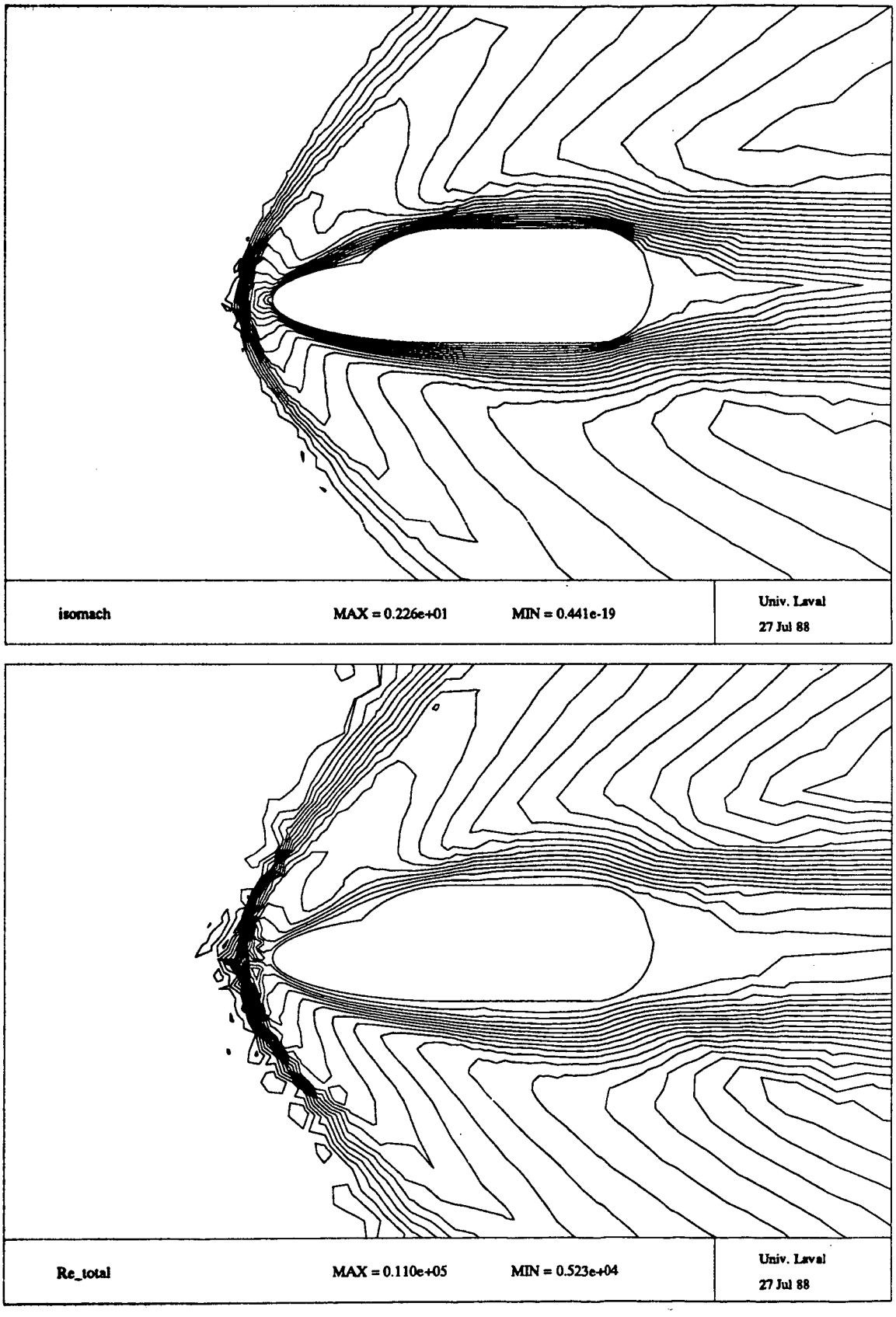

Figure 6: Mach contours and Re number, q-w computation at M=2., Re=10e4.

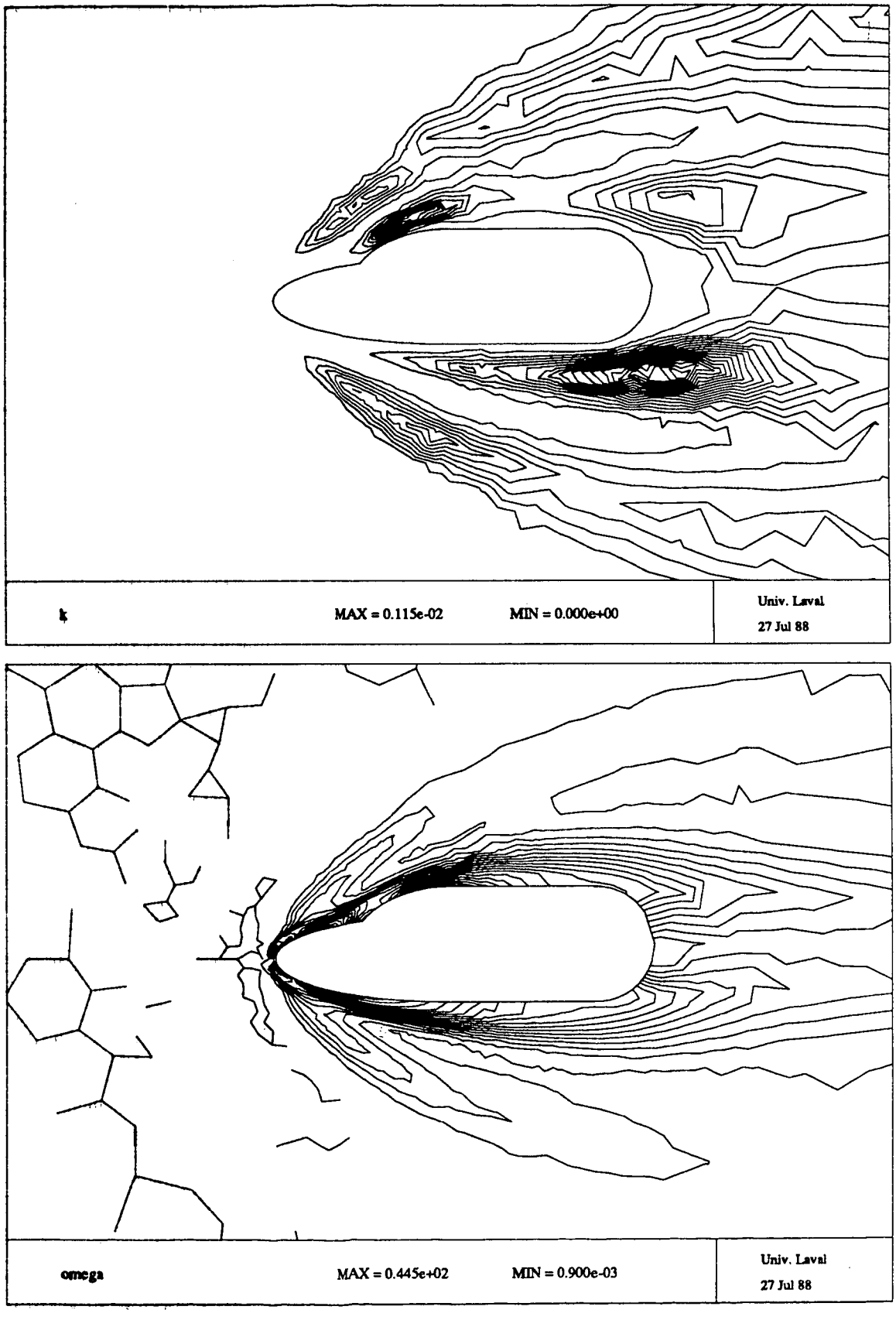

Figure 7: k and w from a q-w computation at M=2.0, Re=10e4.

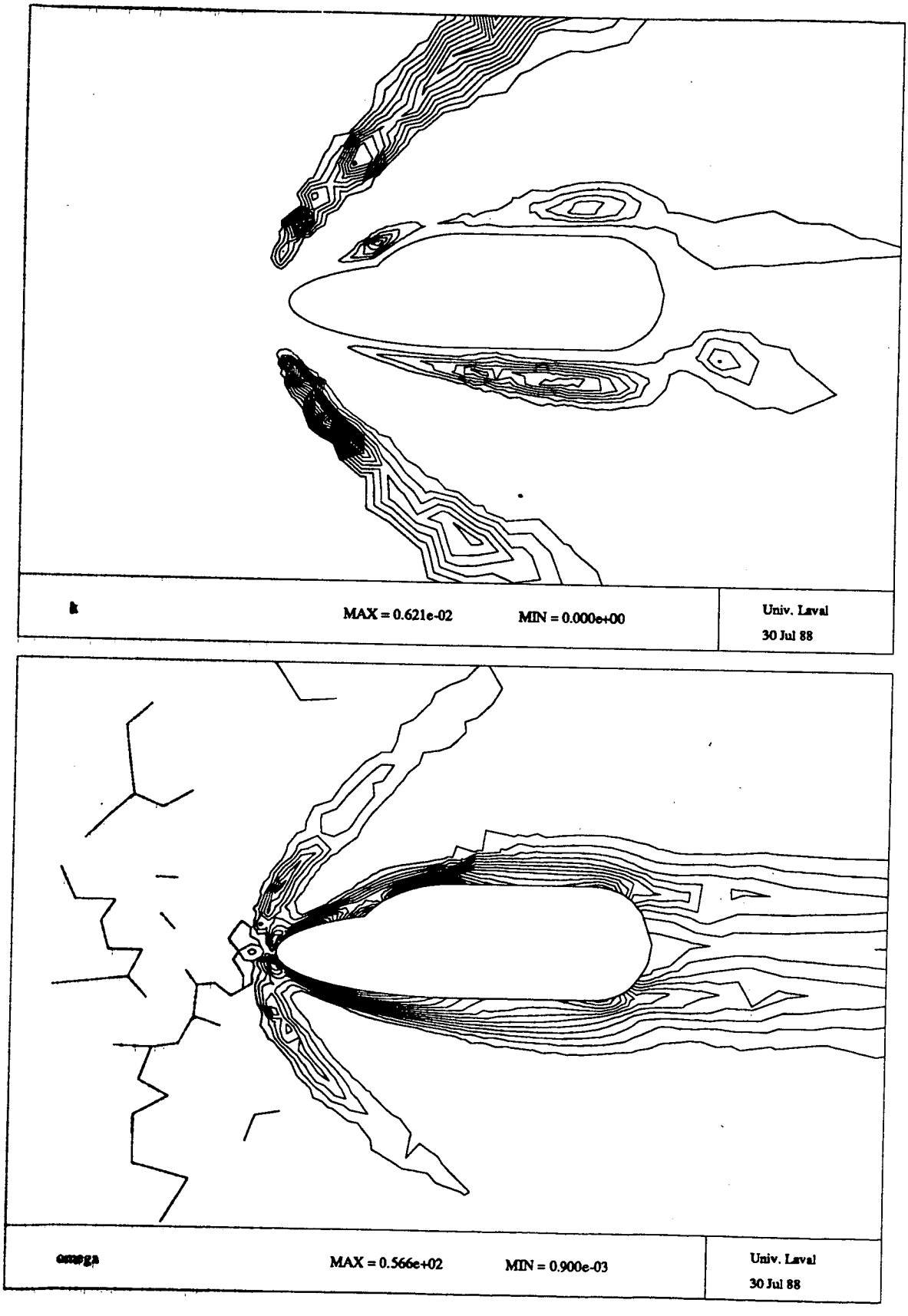

Figure 8: Same as 7 but with a different constant of diffusion in the w equation.

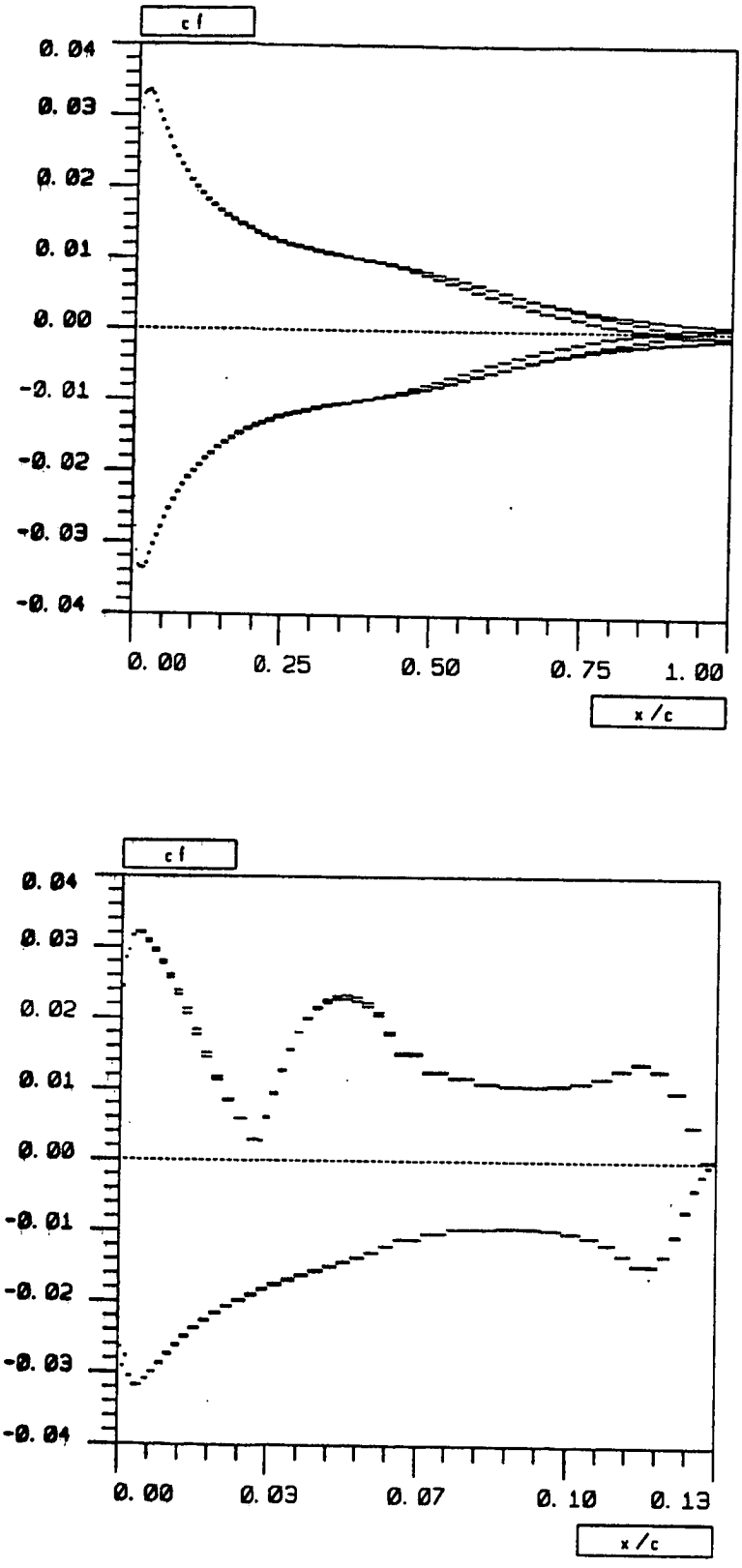

Figure 9: Comparison of friction coefficient, see text for details.

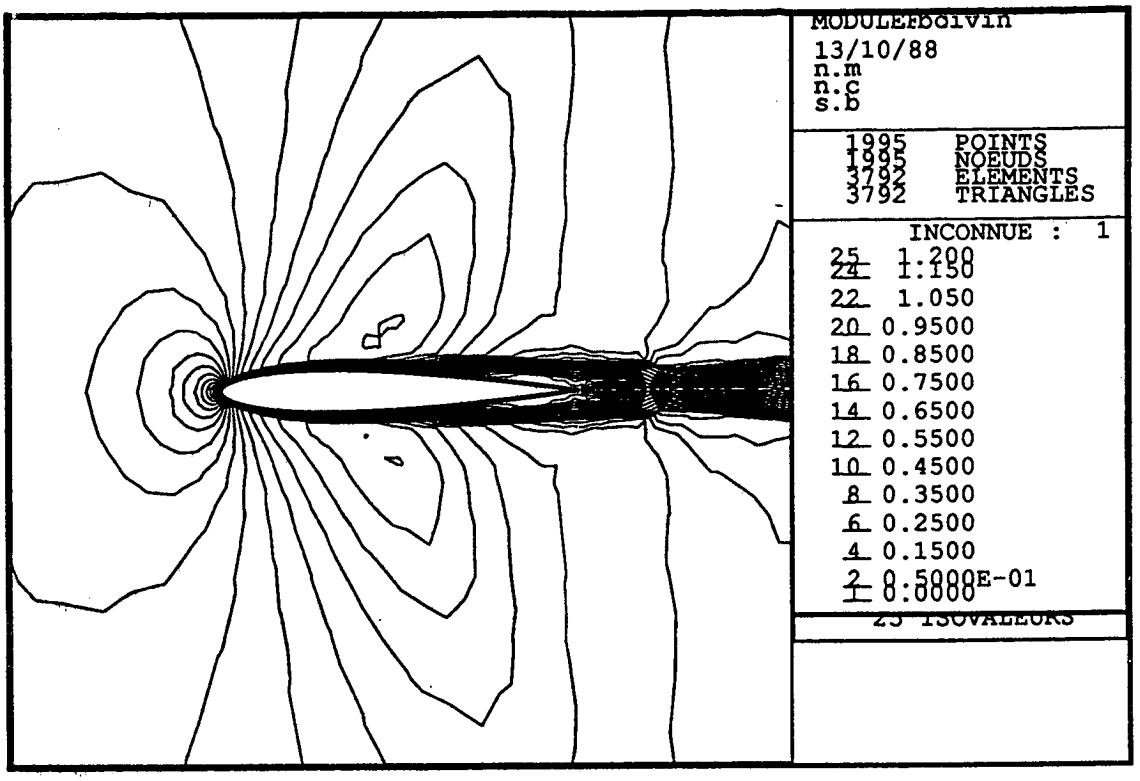

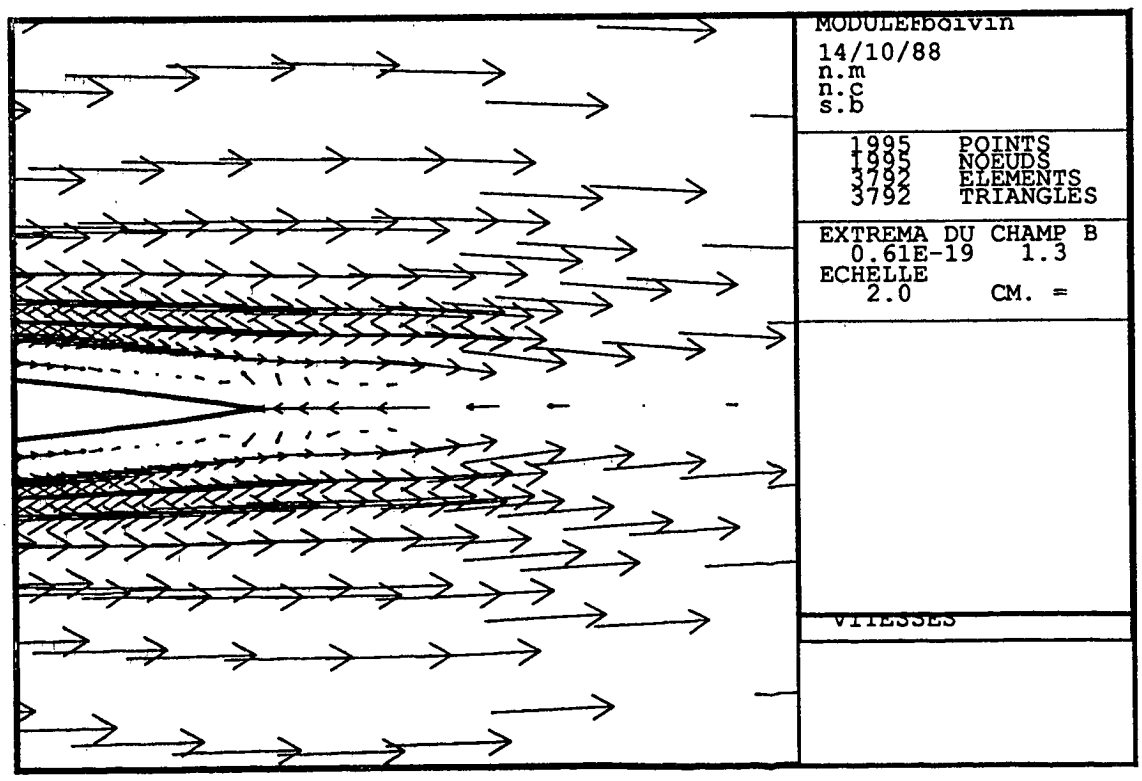

Figure 10: Mach contours and details of the tail flow, M=0.85, Re=10e4.

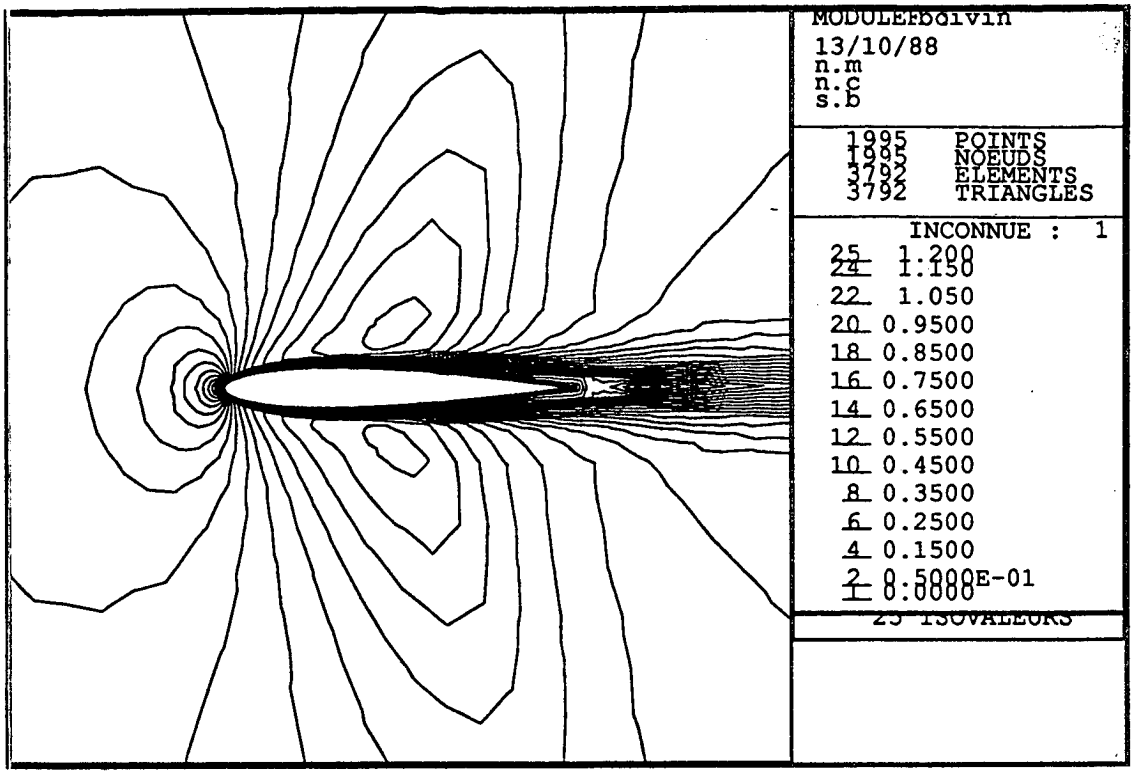

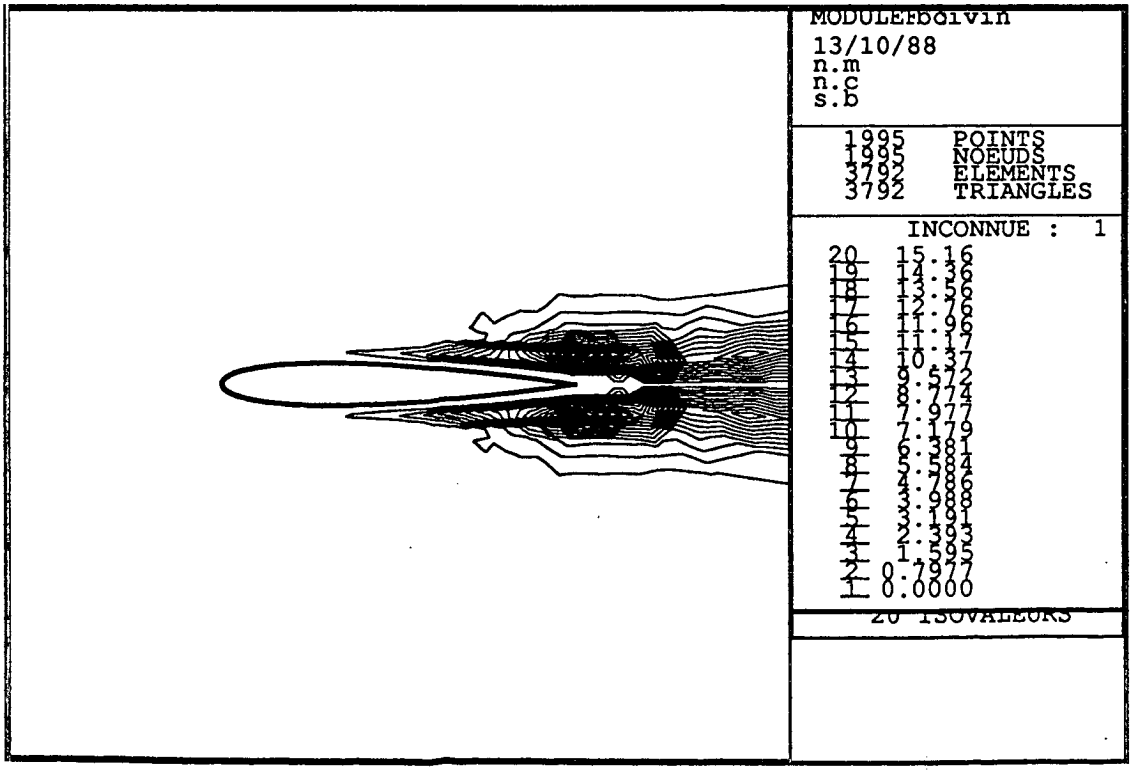

Figure 11: Mach contours and algebraic eddy viscosity, M=0.85, Re=10e4.

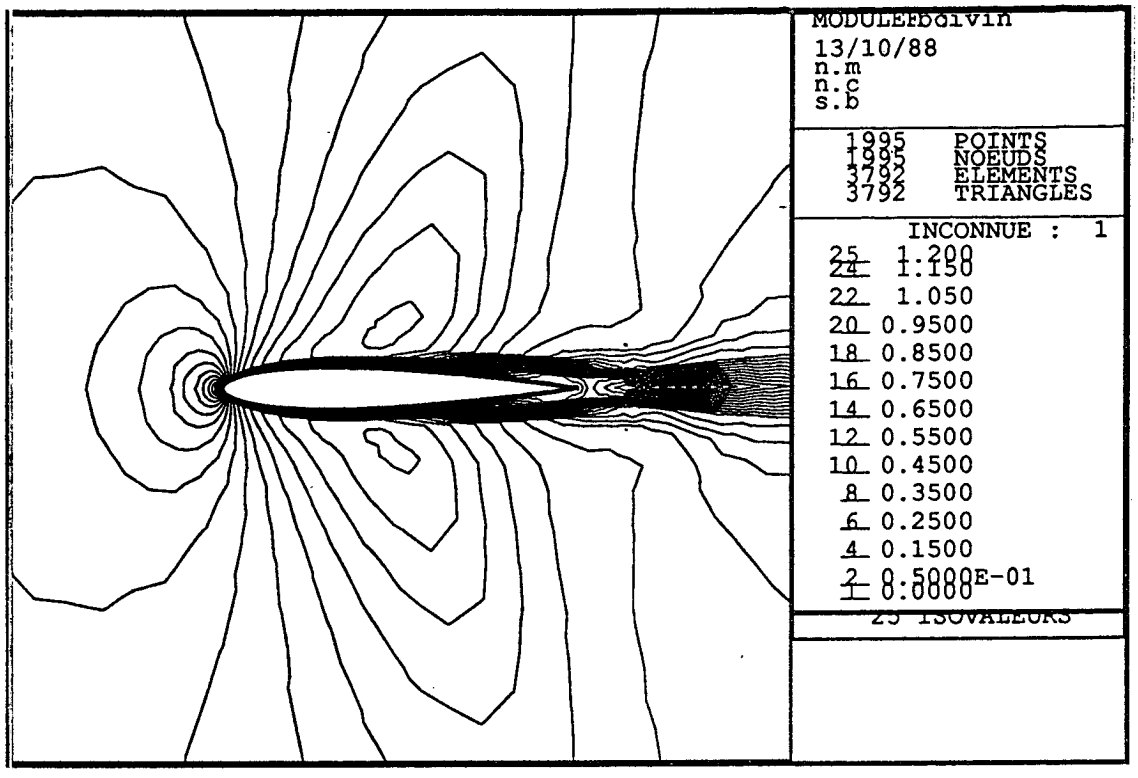

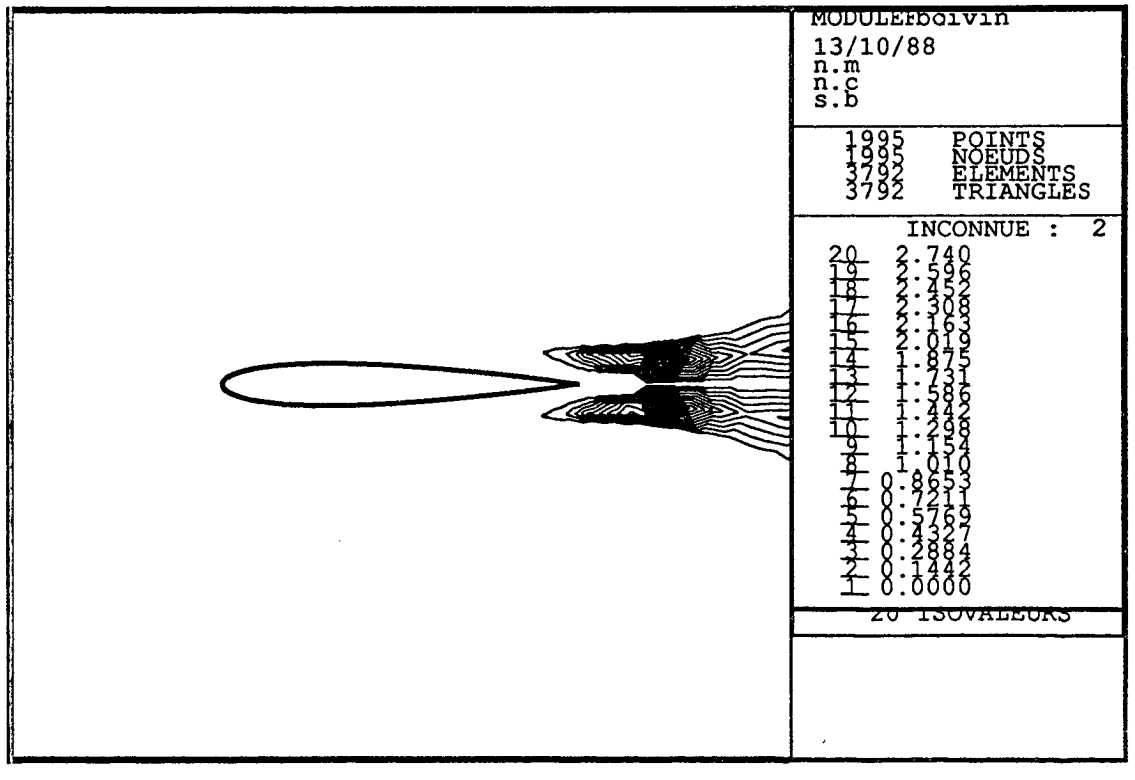

Figure 12: Mach contours and $q-\omega$ eddy viscosity, M=0.85, Re=10e4.